Journal of Mathematical Chemistry 10(1992)329-371

CONFIGURATIONAL DEPENDENCE OF MOLECULAR SHAPE

Gustavo A. ARTECA and Paul G. MEZEY
Department of Chemistry and Department of Mathematics, University of Saskatchewan, Saskatoon, Saskatchewan, Canada S7N 0W0

Abstract

Some of the topological techniques developed for the description of molecular shape are studied, formulated as a problem of embedding nuclei within electronic clouds.

1. Introduction. The shape-configuration relation as an embedding problem

Chemists often think of chemical species at two levels: in terms of their energetic stability and in terms of their three-dimensional shape. It is well understood that the relative energetic stability of some families of nuclear configurations with respect to nuclear rearrangements is the ultimate reason for the existence of chemical species. The three-dimensional nature of molecules is often modeled by fixed or vibrating nuclear configurations where nuclei are treated as formal points in space, and by electron distributions represented as formal molecular bodies (almost classical entities) with well-defined shape.

Strictly speaking, the above view is not compatible with quantum mechanics. Nuclear positions have an uncertainty, though much smaller than that for the electrons, which cannot be neglected. As a consequence of this uncertainty, and the finite size of nuclei, it is not rigorous to represent or define chemical species in terms of point-like nuclear configurations [1,2]. Similarly, formal molecular bodies with sharp boundaries as formal molecular surfaces are only approximations of reality, since electron distributions of molecules have a fuzzy, quantum mechanical character. Once again, we find a conflict with rigorous quantum mechanics, since real molecules have no boundary. If the total electronic density is considered to model the molecular shape, one could talk of a molecular surface, at best, as a fuzzy object. The reasons for choosing a formal molecular surface or a set of molecular surfaces as representatives of molecular shape are often somewhat subjective.

Nonetheless, there are valid empirical reasons for depicting molecules as semiclassical objects with defined shape and size. Empirical parameters representing formal molecular volumes and areas can be measured [3–11]. The interpretation and prediction of these parameters is difficult without the notion of molecular surface [9,11,12], and some classical models provide remarkably good descriptions of the relevant molecular properties.

To a good approximation, one may regard a molecule as a family of nuclei embedded in an electronic cloud. If, following the commonly used terminology, molecular configuration is interpreted as the nuclear configuration, and if the shape of the molecule is regarded as the shape of the electron distribution, then the configurational dependence of molecular shape, the subject of this report, can also be described as a special embedding relation of nuclei immersed in electronic clouds.

This approach is facilitated if one considers the shape of electron distributions as the starting point and uses the concept of three-dimensional molecular shape to define chemical species. The implementation of this approach is perhaps the simplest if the shape characterization is based on formal molecular surfaces, and if some of the geometrical notions are replaced by topological models.

The semiclassical views of molecules can be reconciled with quantum mechanics if the geometrical notion of chemical species as fixed configurations is replaced by a topological one. In this latter approach, species are represented by open sets in configuration space, i.e., by a continuum of configurations. The construction of these continua from the properties of the potential energy surface has been discussed in the literature [13]. On the other hand, the identification of chemical species in terms of shape is a current development. This topic concerns various areas of applied science, such as pharmacology and biochemistry. Synthesis planning and computer-assisted drug design are among the fields where interrelations between energy, shape, and conformational changes are of relevance. The objective of this review if to provide an account of the present status of the study of conformational dependence of molecular shape, and to point out future lines of research.

The organization of this work is as follows. In section 2, we review some concepts relevant to the geometrical and topological treatments of configurational space. In section 3, some current methods for characterizing molecular shape are presented. These methods provide shape codes to identify conformations which are shapewise equivalent. Section 4 presents some results on the interplay between conformational changes and molecular shape. Applications to problems of assessing molecular similarity during a chemical reaction (e.g., the Hammond postulate) are also included in this section. Section 5 is devoted to the comparison between the partitionings of configuration space in terms of the curvature properties of the potential energy surface and in terms of the shape of molecular surfaces. In section 6, we present an extension of previous ideas to the analysis of the interplay between molecular shape and folding in large macromolecular structures. Conclusions and further comments on the development of this field are found in section 7.

2. Geometry and topology of configurational space

The topological model provides a description of molecules radically different from the conventional, geometrical description. Within the geometrical model, the concept of molecular structure is associated with nuclear geometries. By contrast,

in the topological approach, nuclear geometry is replaced by a continuum of nuclear configurations and a reaction path is replaced by a continuum of reaction paths [13]. This picture leads to a new approach to viewing chemical entities, such as molecules and reaction mechanisms [13].

Geometrical and topological approaches have a common feature: as a starting point, they both use the Born–Oppenheimer approach. The topological model, however, provides the means to go beyond the Born–Oppenheimer approximation by replacing individual geometric models by topological families. The topological model provides a classification of nuclear geometries. This is equivalent to a partitioning of the nuclear configuration space. The construction of these regions or domains of configurational space allows one to give a topological structure to such space. One can take advantage of the geometry of the Born–Oppenheimer potential energy hypersurface in order to define such partitionings. As has been shown, and will be briefly reviewed here, one can use the critical points on the surface to give the configurational space a topological structure [13].

For a fixed choice of N nuclei, the family of all nuclear configurations is represented by a metric space M (a set with a distance function defined between its elements), whose elements are the equivalence classes of those configurations which are equivalent to one another under rigid rotations and translation [13]. Chemical reaction paths or conformational changes can be represented by parametrized paths within M. Chemical species (and, in one representation, reaction mechanisms) appear as domains in M. In what follows, we discuss briefly the topologization of this space by introducing a given partitioning.

A natural partitioning can be formulated as follows [13]. Consider a configuration K, $K \in M$, representing a critical point, for example, a minimum of the potential energy hypersurface. One can define an open neighborhood around point K formed by the catchment region of the steepest descent paths leading to K. This region spans the relaxation neighborhood of the critical point: the collection of all those configurations which relax to the given critical point K. In the case of minima of an n-dimensional potential energy hypersurface, these catchment regions are n-dimensional basins, representing qualitatively the domains of molecular vibrations around a stable conformation. If the critical point has an index 1 (a simple saddle point), its catchment region will usually be an $(n-1)$-dimensional ridge, representing the points on all relaxation paths leading to the saddle point. In general, a critical point of index λ (where the Hessian matrix has precisely λ negative eigenvalues) will usually have an associated catchment region of dimension $n-\lambda$. For example, in a two-dimensional surface, a maximum has index $\lambda = 2$, i.e., the critical point itself is its own catchment region. As a result of this analysis, one can associate to every critical point K_i a region $C(\lambda, i)$, which is the so-called catchment region of the critical point K_i; the set of regions $\{C(\lambda, i)\}$ provides a partitioning of space M with the following characteristics:

$$M = \bigcup_{\lambda,i} C(\lambda, i), \tag{1a}$$

$$C(\lambda, i) \cap C(\lambda, j) = \varnothing, \quad i \neq j, \tag{1b}$$

where the set $\{C(\lambda, i)\}$ defines a subbase for a topology of M. Following this approach, one can give a topological structure to the configuration space and then apply topological techniques to the description and characterization of reaction mechanisms on the potential energy hypersurface. This approach has been discussed in the literature in some detail, and the interested reader may find an introduction in ref. [13].

The partitioning of space M can be accomplished by using completely different principles. For example, one can define regions in configurational space characterized by containing configurations sharing a common feature, different from the above. The shape of a molecular surface is one of such properties which can provide an invariance property to classify geometrical arrangements of nuclei [14–22]. Molecular shape (the shape of the electron density) and the conformation of the arrangement of the nuclei are two different concepts. However, it is a known fact that some chemical processes, associated with the molecular shape, show a marked dependence on conformational rearrangements. Here, we study the connection between the molecular shape and the nuclear conformations. In addressing this subject, we will deal with the characterization of molecular surfaces.

The shape of a molecule is a feature of importance when seeking some understanding of molecular properties. The characterization of the shape is a problem of interest in theoretical chemistry, biochemistry, and biophysics, as well as in many areas of applied research. Among them, drug design and synthesis planning are outstanding examples of present importance [23–28].

Molecular shape is usually described by a model surface. Electrostatic potential contours [29–38], isodensity contours [39–41], and Van der Waals surfaces (VDWSs) [3–6, 42–46] are common tools. These surfaces are defined in terms of a single function that is usually based on a physical observable. Descriptions using several functions simultaneously may also have important applications.

Suppose that a molecule, in a given nuclear configuration K, $K \in M$, is represented by a molecular surface, which we will indicate as $G(\boldsymbol{a}, K)$, embedded in 3-space. The discussion applies equally to any kind of model surfaces. In order to specify completely a general surface G, a certain number of parameters must be given, besides the specification of the nuclear configuration K. This set of parameters will be collected formally in a vector $\boldsymbol{a}$. In the case of electronic isodensity contours, a single parameter $\boldsymbol{a}$ is needed, representing the density value along a contour $G(\boldsymbol{a}, K)$. In the case of $G(\boldsymbol{a}, K)$ being a fused-sphere VDWS, the vector $\boldsymbol{a}$ will contain the values of the atomic radii.

Let us indicate now by $\tau(G(\boldsymbol{a}, K))$ a *discrete shape descriptor* of the surface G. An example of a discrete shape descriptor of G is its homeomorphism type (in our case, the number of holes in $G(\boldsymbol{a}, K)$). In general, this latter provides a rather poor characterization, and better descriptors are needed. Molecular topology provides us with a number of alternatives to derive three-dimensional shape descriptors

[14–19,47,48]. The most appropriate choice depends on the model representation chosen for G. The main requirement is that $\tau(G(\boldsymbol{a}, K))$ has to be discrete, i.e., it can be expressed as a finite series of numbers. For example, molecular body and molecular surface are not discrete descriptors, and will not be used directly in our analysis. On the other hand, topological invariants of G, or of surfaces derived from it, are usually discrete. These numbers will not necessarily change with small continuous changes in the parameter $\boldsymbol{a}$ and the nuclear configuration K.

Given a model surface and a shape descriptor, surfaces for different conformations can be classified according to their *shape type*. For fixed values of the generic parameter $\boldsymbol{a}$, a shape descriptor τ associates a shape type with each configuration K. The shape type of K will be indicated as $s(\tau, K)$ and the ith shape type by $s(\tau_i)$. Notice that the classification of configurations according to $s(\tau, K)$ is not relying on molecular symmetry. The shape here is characterized in terms of the molecular envelope surfaces enclosing the nuclei, which can be asymmetrical objects. The shape type $s(\tau, K)$ allows one to define an equivalence relation $\mathrm{s}(\tau)$ between nuclear configurations:

$$K\ \mathrm{s}(\tau)\ K', \quad \text{iff: } s(\tau, K) = s(\tau, K'), \quad K, K' \in M. \tag{2}$$

The elements of the quotient set $M/\mathrm{s}(\tau)$ are the equivalence classes of configurations characterized by their associated molecular surfaces having the same shape features. These equivalence classes are the *shape invariance domains* $S_i(\tau)$ (or "*shape regions*"), in short notation S_i, which provide a partitioning of the configuration space [16, 19]:

$$S_i(\tau) = \{K \in M : s(\tau, K) = s(\tau_i)\} \subset M, \tag{3}$$

with τ_i a particular value (or set of values) of the shape descriptor τ. The concept of shape region in a configurational space constitutes one of the central ideas we shall deal with throughout this work.

The above partitioning of space M into sets $\{S_i\}$ provides a topologization of space M, which is different from the one provided by the catchment regions $\{C(\lambda, i)\}$ of the potential energy hypersurface. In order to study the interplay between molecular shape changes and conformational changes leading to changes in chemical identity, we shall compare these two descriptions of the nuclear configuration space M.

3. Characterization of molecular shape: From graph theory to 3D molecular topology

A number of procedures have been presented recently to describe molecular surfaces. Here, we briefly review several possible sources for such shape descriptors of envelope surfaces. These will be used later to analyze the relations between molecular shape changes and conformational rearrangements.

3.1. RESULTS FROM GRAPH THEORY

Graph theory [49] has been found useful in a great variety of fields, for example in the study of communication and electrical networks, both continuum and discrete statistical mechanics, social and natural sciences, architecture, and linguistics, as well as in chemistry [50, and refs. therein]. In chemical applications, the study has usually been restricted to graphs defined in terms of the classical skeleton of atoms and bonds as vertices and edges, respectively, of the graphs [51–59]. These graphs are *conformation independent.* A first approach to conformationally dependent chemical graphs has been presented recently [60]. Nevertheless, graphs defined only in terms of connectivity of atomic nuclei are not in general a sufficiently discriminating tool for shape and conformational analysis. On the other hand, graphs defined in terms of three-dimensional shape features of the formal molecular *body* can overcome this difficulty.

A topological characterization of a molecular surface can be given in terms of various graphs (*shape graphs and incidence graphs* [18], *as well as seeing graphs* [61]). The construction of a graph can be based on partitioning of the molecular surface into subregions, defined in terms of their curvature relative to a reference value [14,15,18]. Twice continuous differentiability of the surfaces is then a requisite. The latter condition is not fulfilled by all molecular surfaces (for example, a VDWS does not meet this condition). In the case of seeing graphs, differentiability is not a requisite [61].

A fused-sphere VDWS is the simplest model of a molecular surface that can be considered of actual interest for applied shape research. The VDWS for an N-atomic molecule is defined by two sets. The set C_x specifies the position vectors for the nuclei:

$$C_x = \{x_1, x_2, \ldots, x_N\}, \qquad x_i \in \mathbb{R}^3, \tag{4a}$$

and the set C_r contains the atomic Van der Waals radii r_i corresponding to the atomic spheres,

$$C_r = \{r_1, r_2, \ldots, r_N\}, \qquad r_i \in \mathbb{R}^1. \tag{4b}$$

The set C_x defines a molecular configuration. This can be represented by an element K of the reduced nuclear configuration space M [13]. The VDWS, represented by a function G, is the object formed by the envelope of the superposition of interpenetrating spheres. We formally indicate the surface as $G(C_r, K)$, where the set C_r of atomic radii plays the role of vector $\boldsymbol{a}$ (cf. section 2).

A molecular graph determined only by the nuclear positions will not appropriately describe the molecular shape. A nontrivial graph must be built, indeed, by considering explicitly the details of the interpenetration of atomic spheres. In ref. [62], a class of such graphs is proposed. The construction of graph $g(G(C_r, K))$ is based on defining a number of subsets of $G(C_r, K)$. These sets contain the points on the

VDWS arranged according to the precise number of atomic spheres to which they belong simultaneously. Let $C_r^{(k)}$ be a subset of C_r, $C_r^{(k)} \subset C_r$, containing k different elements, $k \leq N$. A subset $D_k \subset G(C_r, K)$ containing all the points belonging simultaneously to exactly k spheres is defined as [62]:

$$D_k = \{r \in G : \exists C_r^{(k)} \subset C_r,\ \forall r_i \in C_r^{(k)}, \|r - x_i\| = r_i,\ x_i \in C_x\},\quad k = 1, 2, \ldots, m^*, \tag{5}$$

with $\| \ldots \|$ the norm of a vector, and m^* the maximum number of spheres to which a point on G may belong. A set D_k may be pathwise disconnected. We indicate with $D_k^{(i)}$ the ith among the n_k maximum connected subsets of D_k,

$$D_k = \bigcup_{i=1}^{n_k} D_k^{(i)},\quad D_k^{(i)} \cap D_k^{(j)} = \varnothing,\quad i \neq j. \tag{6}$$

The vertices of the graph, collected in vertex set $V[g(G(C_r, K))]$, are these maximum connected components:

$$V[g(G(C_\rho, K))] = \{D_k^{(i)},\ i = 1, 2, \ldots, n_k;\ k = 1, 2, \ldots, m^*\}. \tag{7}$$

In order to define the edges of the graph, we observe the following properties:

(i) A typical nonempty set $D_1^{(i)}$ contains an infinite number of points. Its set-theoretical closure, $\mathrm{clos}[D_1^{(i)}]$, must contain points of D_2 whenever $\mathrm{clos}[D_1^{(i)}] \neq D_1^{(i)}$.

(ii) A nonempty set $D_2^{(i)}$ contains either an infinite number of points or else a single one. Its closure can have points in D_p, $p \geq 3$.

(iii) A nonempty set $D_p^{(i)}$, $p \geq 3$, can have only a single point, with the exception of the degenerate cases.

Taking into account the above properties, one can define the edges by using the nodes $D_k^{(i)}$ in a hierarchy according to k. To this purpose, we define a neighbor relation. We first define an index $\kappa(k)$ as follows:

$$\kappa(k) = k,\ \text{if } k < 4,\quad \text{and}\quad \kappa(k) = 3,\ \text{if } k \geq 4. \tag{8a}$$

The neighbor relation is given by [62]:

$$N(D_k^{(i)}, D_{k'}^{(j)}) = \begin{cases} 1, & \text{if: } \mathrm{clos}[D_k^{(i)}] \cap \mathrm{clos}[D_{k'}^{(i)}] \neq \varnothing, \text{ and } |\kappa(k) - \kappa(k')| = 1, \\ 0, & \text{otherwise.} \end{cases} \tag{8b}$$

Finally, the edges of the graph, collected in set $E[g(G(C_r, K))]$, are determined by the set of pairs $(D_k^{(i)}, D_s^{(j)})$ that have a nonzero neighbor relationship:

$$E[g(G(C_r, K))] = \{(D_k^{(i)}, D_s^{(j)}) : N(D_s^{(i)}, D_k^{(j)}) = 1\}. \tag{9}$$

This neighbor relation can also be expressed in terms of the "symmetric strong neighbor relationship" of ref. [13], that would lead to exactly the same set of edges. The neighbor relation (8) differs from the usual incidence relation of cells of dimension two, one, and zero obtained after a cellular decomposition of a surface. In our case, a set $D_2^{(i)}$ can either be a one-dimensional or a zero-dimensional cell.

The construction of the graph $g(G(C_r, K))$ (the so-called "Van der Waals graph", VDWG) is rather simple and it allows a characterization of both shape and nuclear conformations. Domains in configurational space can then be classified according to the invariance of the VDWG of their associated nuclear configurations [62]. In other words, the VDWG can provide a shape descriptor $\tau(g(G(C_r, K)))$ that can be used in the definition of shape regions.

Other types of graphs, defined in terms of the cross sections of molecular surfaces have also been proposed [63].

3.2. TOPOLOGY OF MOLECULAR SHAPE: ANALYSIS OF MOLECULAR SURFACES

A molecular surface can be defined as an "isoproperty surface", for example, as an isodensity surface or an isopotential surface, with respect to the "properties" of electronic density and electrostatic potential, respectively. For convenience in the topological analysis, it is advantageous to regard a molecular surface as a boundary G of a level set F of the physical function $\rho(\boldsymbol{r})$ of interest, with $\boldsymbol{r}$ a position vector in 3-space, $\boldsymbol{r} \in \mathbb{R}^3$, and a chosen value a [14,15]. (A level set $F(a)$ is the collection of all those points of the space where the value of function $\rho(\boldsymbol{r})$ is greater than a threshold a.) Contour surfaces serve as models for the molecular envelopes. A contour surface is given as the boundary of the level set of a function, that is,

$$G(a, K) = \{\boldsymbol{r} \in \mathbb{R}^3 : \rho(\boldsymbol{r}) = a\}. \tag{10}$$

This function $\rho(\boldsymbol{r})$, which depends parametrically on the configuration K, can be the total electronic density [37–41], the molecular electrostatic potential [29–36], or a formal function defining the Van der Waals envelope surface [3–6,42–46,64].

A possible characterization of surface $G(a, K)$ requires the introduction of a local system of coordinates at every point of the surface. The classification of points on the surface according to the local curvature refers to such a local coordinate system. A set of three orthogonal vectors is attached to every point $\boldsymbol{r}$ on the surface $G(a, K)$. One of these vectors is the gradient; the other two are orthogonal to each other and to the gradient, and they span a plane tangent to the surface at point $\boldsymbol{r}$.

Let $\boldsymbol{u}_1(\boldsymbol{r})$ and $\boldsymbol{u}_2(\boldsymbol{r})$ be two orthogonal vectors, constituting a basis set for the plane tangent to $G(a, K)$ at point $\boldsymbol{r}$. Let the components of the vectors be given as $\boldsymbol{u}_i(\boldsymbol{r}) = (u_{ix}, u_{iy}, u_{iz})$, with u_{is} real numbers, $i = 1, 2$, $s = x, y, z$. If ∇ represents the gradient operator with respect to the original Cartesian frame, that is, $\nabla = (\partial/\partial x, \partial/\partial y, \partial/\partial z)$, then the matrix elements of the two-dimensional Hessian matrix $\mathbf{H}$ at point $\boldsymbol{r}$ are given as follows:

$$H_{ij}(\boldsymbol{r}) = \boldsymbol{u}_i(\boldsymbol{r})^{\mathrm{T}}\, {}^3\mathbf{H}(\rho)\boldsymbol{u}_j(\boldsymbol{r}), \qquad i = 1, 2,\ j = 1, 2, \tag{11}$$

where ${}^3\mathbf{H}(\rho) = \nabla\nabla\rho(\boldsymbol{r})$ is the 3×3 matrix of second Cartesian derivatives of the density function $\rho(\boldsymbol{r})$, evaluated at point $\boldsymbol{r}$. The two directions $\boldsymbol{u}_i(\boldsymbol{r})$, $\boldsymbol{u}_j(\boldsymbol{r})$ orthogonal to the gradient can be chosen easily using a conventional orthogonalization method. Using eq. (11), one may compute the eigenvalues of the local Hessian matrix corresponding to the canonical curvatures. By means of these eigenvalues, the local curvature of the surface can be characterized and the corresponding shape groups (*vide infra*) can be computed.

Let h_1 and h_2 be the two eigenvalues of $\mathbf{H} = (H_{ij})$. Let b be a real constant, $b \in \mathbb{R}$, that will be taken as a reference curvature. A surface $G(a, K)$ is then partitioned into curvature subsets in the following way [15]:

(i) If both eigenvalues of the local Hessian matrix are smaller than b, i.e., $h_1 \leq h_2 < b$, then the point $\boldsymbol{r}$ is said to belong to a $D_2(b)$ subset. The subscript in the notation makes reference to the fact that *two* eigenvalues are smaller than b. When $b \leq 0$, then a D_2 region is convex.

(ii) If $h_1 < b \leq h_2$, i.e., when only *one* eigenvalue if smaller than b, then the point $\boldsymbol{r}$ is said to belong to a $D_1(b)$ subset. In the particular case of $b = 0$, the D_1 region is a saddle-type subset of $G(a, K)$.

(iii) When $b \leq h_1 \leq h_2$, then the point $\boldsymbol{r}$ belongs to a $D_0(b)$ subset. This region is concave in the case $b \geq 0$.

Let $D_\mu^{(i)}(b)$ be the ith subset of $G(a, K)$ with curvature characterized by μ, with $\mu = 0$, 1, or 2. The number and type of these regions on the contour surface depend on the parameter b, as well as on a. The subdivision of surface $G(a, K)$ into the above curvature domains provides a proper partitioning, needed for a topological characterization. Let us now define a truncated surface $G_\mu(a, b)$, obtained from $G(a, K)$ by the truncation of all the $D_\mu(b)$ subsets, for a fixed index μ:

$$G_\mu(a,b) = G(a,K) \setminus \bigcup_i D_\mu^{(i)}(b), \qquad a, b \in \mathbb{R},\ \mu = 0, 1, \text{ or } 2. \tag{12}$$

For the sake of simplicity in the notation, the configurational dependence will be omitted in the truncated surfaces. The truncated surface $G_\mu(a, b)$ can be formed by one piece or several disjoint pieces (maximum connected components). Each of these truncated surfaces can be characterized by topological invariants. For example, the homology groups [65] $H_\mu^j(a, b)$, and their ranks $b_\mu^j(a, b)$, the Betti numbers [65], with $j = 0, 1, 2$, provide a simple method for characterization of $G_\mu(a, b)$ [14–16, 18, 19]. The *shape groups* of $G(a, K)$ are the homology groups of various truncated surfaces $G_\mu(a, b)$ [14, 15]. The methodology based on characterizing the surface $G(a, K)$ in terms of its shape groups is termed the shape group method (SGM). An alternative formulation of the SGM for nondifferentiable surfaces (e.g., fused-sphere VDWSs) has also been developed [17, 18, 66, 67].

If a surface $G_\mu(a, b)$ is formed by several pieces, one can consider it as a single topological entity, or one can compute the Betti numbers of its maximum connected components. For the sake of a simple classification, we will here follow this latter alternative. The Betti numbers are integer numbers, and they provide a concise, but informative characterization of the surface $G(a, K)$. The topological meaning of these groups, as well as their actual computation from a given surface, has been the subject of several studies [14–19], and will not be repeated here.

For fixed μ and j values, the Betti numbers may change at some precise values of the parameters a and b. One may characterize the entire function G by describing the changes of $b_\mu^j(a, b)$ (of fixed j and μ) in the parameter plane a, b. This construction is an (a, b)-parameter map of the function G. Various algorithms for the actual construction and analysis of these maps for model electronic density functions have been proposed [68].

3.3. TOPOLOGY OF MOLECULAR SHAPE: ANALYSIS OF MOLECULAR SPACE CURVES

The structure of large molecular systems can be described considering different levels of organization. The possibility of several scales for viewing the shape features of macromolecules allows one to employ different types of models. Molecular surface models (such as the hard-sphere Van der Waals models) are often used to represent a molecule. However, it is cumbersome to analyze the shape features of such models for molecules with a very large number of atoms. Alternative approaches are needed in these cases.

One of the commonly used models in protein studies is the construction of macromolecular ribbons, for example, based on the method of Richardson [69–72]. In Richardson's model, α-helices are represented by solid cylindrical helices of solid ribbons, β-strands are shown as thick arrows, whereas the nonrepetitive loops connecting β-strands and helices are modelled by thick "strings".

These models are used for graphical displays of the macromolecular structure. Usually, the description of the shape features of these molecular ribbons is based on subjective visual inspection. This procedure is somewhat unreliable when one needs precise shape comparison, as is the case when studying differences between molecules or a given molecule undergoing conformational changes such as folding. The methods discussed above appear cumbersome, although they are useful if one needs to pay attention only to certain local features of some part of the molecular surface. On the other hand, a study of global shape features of a ribbon model of a macromolecule can rely on alternative methods. For example, it is possible to assign a space curve (a one-dimensional object) to the ribbon [73]. A number of methods have been proposed in the literature to characterize these space curves [74–79]. In a recent work, we have proposed a new approach to describe folding and motion in macromolecular systems by characterizing their associated molecular space curves [80,81]. The characterization of this curve can be performed by defining three preferential observational (orthogonal) directions, and by projecting the curve

onto planes defined by pairs of the above directions. The projections can be characterized in terms of plane graphs [49], taking into consideration the overcrossings of the spave curve.

Moreover, a class of knots [82] can be built from the projected view of the space curve. These knots can be characterized by polynomials, which provide an alternative algebraic characterization to the original ribbon. In section 6, we discuss this approach in more detail, and we present some new results on characterization of protein folding by a projection-independent method.

4. Relations between conformational changes and molecular shape

The reduced nuclear configuration space M is convenient to describe conformational rearrangements and chemical reactions. As mentioned in section 2, its points represent equivalence classes of nuclear configurations which are transformable into one another by translation and rigid rotation.

The partitioning of space M, based on various properties such as curvature of a potential energy hypersurface or the molecular shape, has been discussed in detail [13,16,18, and original references therein]. In this section, we discuss the analysis of molecular shape changes along reaction paths by using the ideas of the partitioning of space M into shape regions.

4.1. DYNAMIC SHAPE SPACE

One may analyze the interrelations between molecular shape and nuclear conformations by considering "realistic" molecular surfaces, such as electronic isodensity contours. In this case, one can resort to analyzing every nuclear configuration in terms of its associated molecular surface, whose shape can be characterized in terms of the (a, b)-parameter map discussed in section 3.2. For a given configuration, the shape groups of a surface depend on the parameters a and b, the level set and reference curvature values, respectively. If the configuration changes only slightly for a given set of values a and b, the shape groups of a surface may remain invariant. The relation between configuration and shape group changes provides a measure of the influence of nuclear rearrangements on molecular shape.

One can provide a thorough description of the shape features for the entire configurational space M upon considering a product space $\mathcal{D}$, the so-called dynamic shape space [18]:

$$\mathcal{D} = P \otimes M, \tag{13}$$

where P is the parameter space of parameters a and b. Notice that a partitioning of space M in terms of potential energy catchment regions leads to a partitioning of the dynamic space $\mathcal{D}$. If $C(\lambda, i)$ represents a catchment region, then there will in general exist a domain $\mathcal{D}_{ij} \subset P \otimes C(\lambda, i)$, where configurations belonging to the

catchment region possess the same shape features, described by some shape invariant $\tau_j(G(a, K))$. Exceptionally, if $\mathcal{D}_{ij} = P \otimes C(\lambda, i) = d_i$, then all the catchment region would possess the same shape descriptor for all values of a and b. This is unlikely to be a common situation, unless one restricts the values of a and b to some special ranges [18].

4.2. CONCEPT OF SHAPE INVARIANCE REGIONS OR "SHAPE REGIONS" IN SPACE M

In the following discussion, we shall consider fixed values for parameters a and b. Suppose that a molecule, in a given nuclear configuration K, $K \in M$, is represented by a molecular surface, which we will indicate as $G(a, K)$, embedded in 3-space. Our goal is to characterize the changes in shape of $G(a, K)$, in particular when K changes along a given reaction path.

In a first approximation, $G(a, K)$ can be taken as a VDWS. As discussed in section 3.1, the molecular surface is denoted by $G(C_r, K)$, with C_r the set of atomic radii. VDWSs can be characterized by means of graphs and algebraic groups. The result provided by any of these approaches will be indicated as a generic shape descriptor $\tau(G(a, K))$. It must be emphasized that the characteristic shape graphs and shape groups of a VDWS [62,66], although related to those discussed in previous sections, are not the same as those of a differentiable contour surface.

In general, a configurational change leads to a different element K of the configurational space M. If the change in the nuclear geometry introduces an essential modification in the shape of the molecular envelope surface, then there will be a change in the corresponding topological descriptor $\tau(G(a, K))$. If the shape descriptor is taken as the Van der Waals graph, then its changes can be reflected in the number of vertices and in the edge connectivity.

One may focus on the changes in shape along a specified reaction path [16,21,22,62]. Such a path can be viewed as a continuous assignment of numbers from the unit interval I to the points K of configurational space M. This assignment can be regarded as a parametrization of the path, the parameter taking the role of a reaction coordinate changing its value from 0 to 1 along the path [13]. Using the topological terminology, the path is a mapping between topological spaces:

$$P : (I, T) \rightarrow (M, T'), \quad I = [0, 1], \tag{14}$$

where T and T' are usually taken as the respective metric topologies. (For alternative, chemically motivated topologies for M, see ref. [13].) According to (14), the paths can be parametrized as $P(t)$ by means of a single variable t, $t \in [0, 1]$, and the shape of the molecular surface can be regarded as a function of t. In what follows, we denote a molecular surface associated with a given point along the reaction path as $G(a, P(t))$. We use the following convention: $G(a, P(0))$ represents the molecular surface for the reactant, whereas $G(a, P(1))$ stands for the molecular surface of the product. The symbol $P(t)$ may mean the entire path, or simply the configuration of reaction coordinate value t.

The shapes of two molecular surfaces, corresponding in general to two distinct nuclear configurations K and K', will be regarded equivalent if and only if they possess the same shape descriptors.

If the surface is modelled by a VDWS, then one may choose the following two shape descriptors [17,20,66]: two ordered sets ϕ and χ. The set $\phi = \{\phi_0, \phi_1, \phi_2, \ldots\}$ contains the list of the numbers of various polygonal spherical faces occurring on the VDWS (an n-type face, $n \geq 1$, being a section of a sphere with a boundary formed by a sequence of n spherical adjoining arcs; for $n = 0$, one has an isolated sphere). The set $\chi = \{\chi_0, \chi_1, \chi_2, \ldots\}$ contains the Euler–Poincaré characteristics [65] (topological invariants) of the surface G_n, obtained upon truncating from surface G the ϕ_n n-type faces present. In most cases, G_n is topologically distinguishable from the original surface G. The computation of these discrete shape descriptors can be performed easily in a totally automated way [17,20].

The equivalence in shape for two such molecular surfaces is then expressed as:

$$G(C_r, K) \approx G(C_r, K') \Leftrightarrow \phi(G(C_r, K)) = \phi(G(C_r, K')), \quad \text{and}$$

$$\chi(G(C_r, K)) = \chi(G(C_r, K')). \tag{15}$$

The configuration space M can therefore be partitioned into subsets including all those configurations having equivalent VDWSs. A shape invariance domain in configuration space, or simply a "shape region" [16–18], is then given as:

$$S_i(\rho) = \{K \in M : G(C_r, K) \approx G(C_r, K') \approx G_i\}, \quad S_i \subset M, \tag{16}$$

where $K' \in M$ is some reference configuration having the ith shape type.

A domain S_i in configuration space, a so-called *shape region*, represents *the equivalence class of all configurations having the common feature of possessing an associated molecular surface with the same shape characteristics* [16]. Shape regions are entities defined in terms of a selected shape descriptor, hence they are not absolute entities, in contrast with their counterparts, the *catchment regions* of the potential energy surface. In the first place, a shape region is defined in terms of a molecular surface, which can be represented by many model surfaces. Electronic isodensity contours are only one of a number of possible choices. Secondly, a shape region is dependent on the descriptor used for the molecular shape. Shape being a concept without a unique definition makes any attempt to define "absolute" shape regions in configuration space subjective. In this sense, the notion of shape region refers to an entity without the clear physical meaning one finds in catchment regions. One can associate a *chemical species* to catchment regions in configurational space, linking them to experimental information. On the other hand, a similar association of shape regions to experimentally measurable entities seems unlikely. Nevertheless, there exist approximate relationships between the two types of partitionings of the configurational space which can be physically meaningful. For instance, the larger

the number of shape regions contributing to a given catchment region, the greater variety of chemical behavior is expected from the associated chemical species. Accordingly, the interrelation among these shape-based and potential-energy-based partitionings of space M may throw some light on the reactivity of a given chemical species. The number of types of shape regions S_i will depend on the molecule considered. The occurrence of shape invariants associated with chemical species will be discussed in the following sections.

Summarizing the above, the shape-region partitioning of M provides a characterization of the relationships between changes in molecular conformations and molecular shape. In a following section, we shall compare this partitioning in terms of molecular shape with that of catchment regions, that is, the potential-energy-based definition of chemical species.

Considering fused-spheres Van der Waals surfaces, an additional degree of freedom is introduced if one allows a uniform scaling in the choice of the set of atomic radii C_r. Continuous change in the atomic radii can mimic, in a first approximation, the fuzzy boundary of the three-dimensional molecular "body". In principle, two different shape regions $S_i(\boldsymbol{r})$ and $S_j(\boldsymbol{r})$, $i \neq j$, can partly overlap when a dilation of the atomic radii is allowed. This situation would imply that, due to the fuzzy nature of the molecular boundary, the generic surfaces G_i and G_j will have the same shape description. We shall comment on these relations between molecular conformations, atomic radii, and molecular surfaces. Due to the high dimensionality of the problem, we will restrict the treatment to a small subset of molecular configurations.

4.3. CHARACTERIZATION OF RELAXED CROSS SECTIONS

Along a given path $P(t)$ connecting two configurations $K_0 = P(0)$ and $K_1 = P(1)$, the molecular shape can undergo various changes. If the molecule is represented by a VDWS, some of these changes can be described as a modification in the shape descriptors $\chi(K)$ and $\phi(K)$. If one follows a path $P(t)$, the characteristic $\chi(K)$, with $K \in P(t)$ as a function of t, could change at a number of critical values of $t \in I$, representing "shape transition points" in a topological sense [16,17,20–22]. Within each shape region, any conformational rearrangement leads to no essential modification in the shape of the molecular envelope, as represented by the given shape descriptor.

In this work, we limit ourselves to the simplest systems: two-dimensional conformational problems. That is, we consider only a subset Φ_2 of space M, the points $K(p)$ of which can be labelled by a pair p of two internal coordinates, $p = (\varphi_1, \varphi_2)$. This subset is an *approximate relaxed cross section of the configurational space*, a subset where a subset of coordinates are taken as explicit variables, while the potential energy function is minimized over all other coordinates. In our case, the selected internal coordinates will be the two torsion angles φ_1 and φ_2, defining the set Φ_2:

$$p = (\varphi_1, \varphi_2), \quad K((\varphi_1, \varphi_2)) \in \Phi_2. \tag{17}$$

In a shorthand notation, we shall refer to configuration $K(p)$ by its representation p in the cross section. Such subsets Φ_2 are physically relevant for many applications. In general, torsional motions can be easily separated from other vibrational motions for energetic reasons. The SGM allows one to introduce a discrete description over a continuum of surfaces, as is the case of the VDWSs $G(\boldsymbol{a}, p)$ with $K(p) \in \Phi_2$. Shape invariance domains S_i in Φ_2 represent two-dimensional projections of the conformational domain corresponding to the shape regions in M. In general, the planar curves representing the projections of reaction paths will pass through different shape regions when connecting different critical points.

The energy–molecular shape interrelations in 2D conformational maps provide some clues to the expected behavior for larger systems. Later, we discuss the relation between the changes in potential energy, shape, and nuclear rearrangements using some hydrogen-shift reactions as examples.

4.4. ANALYSIS OF SIMILARITY MEASURES FOR CHEMICAL SPECIES ALONG REACTION PATHS

As discussed above, reactions paths can be represented as trajectories in space M. They can be described parametrically in tems of a single variable taking values from the unit interval [0, 1], 0 corresponding to the reactant, 1 to the product (cf. eq. (14)). In general, in space M the paths can pass over different shape regions. Accordingly, segments of the path will correspond to different shape types. These distinct shape types represent the labels identifying distinct shape regions, describing essential changes in the shape of the molecular envelope during a configurational rearrangement.

Reaction paths connecting critical points are the most important. Several results are known regarding the molecular symmetry along these reaction paths, which are all based on point group and framework group theory (see refs. [13,84–86]). In our case, we are not dealing with nuclear geometries, but with three-dimensional envelope surfaces. Results holding for the point group symmetries along the path hold also for the symmetry of the molecular surfaces, since a nuclear conformation and its corresponding molecular surface have at least the same point symmetry group, or possibly higher in the case of accidental coincidence of certain surface parameters [87].

However, if the molecular shape is described at a level other than point symmetry group theory, then some additional features can occur along the path [21,22]:

(i) Consecutive segments of the path not containing critical points conserve the point group symmetry, but not necessarily the shape type.

(ii) Critical points at the extremes of the path ($P(0)$ and $P(1)$) with different point groups can have the same shape type.

(iii) Critical points at the extremes of the path ($P(0)$ and $P(1)$) with the same point groups can have different shape type.

By analyzing changes along a reaction path, one can compare the results with an earlier approach based on defining the species along the reaction path in terms of catchment regions. (Regarding some new results on symmetry theorems for catchment regions and reaction paths, see ref. [86].) In this latter case, a steepest descent path connecting a saddle point of type $\lambda = 1$ with a minimum on the potential energy hypersurface [13] involves only two formal "species": the stable species at the minimum and a transition structure. All points of the reaction path, except the initial point, belong to the catchment region of the minimum. On the other hand, if one follows the molecular shape changes along the path, then the results can be quite different. For example, a segment of the path with nonzero length, and not just a point, will usually be associated with the transition structure. This seems a reasonable physical picture, since nuclear configurations within a small neighborhood of *any* critical point will not be very different from the critical points themselves and, consequently, the corresponding configurations are likely to exhibit very similar molecular shape features.

The existence of a finite number of distinct molecular shape types along the reaction path provides a measure of similarity between nuclear conformations. This is used in ref. [21] to present an alternative interpretation of the quantitative Hammond postulate in terms of the shapes of molecular surfaces. In this case, a graph-theoretical characterization of a continuum of VDWSs was used for studying simple triatomic isomerizations and collisional reactions. If the surface is chosen as a VDWS and its shape descriptor as the graph $g(G(C_r, K))$, then a *molecular form will be represented by the equivalence class defined by a common graph* $g(G(C_r, K))$ *in the configuration space*. Alternatively, the shape characterization can be performed by applying the method developed in ref. [66] and commented on in section 4.2.

In the usual "quantitative" form, the Hammond postulate states that, along a reaction path, conformations differing slightly in their energy content must be structurally similar and easily interconvertible to each other [88–95]. This is commonly taken as implying that endothermic reactions have "late" transition structures (i.e. ones more similar to the products), and that exothermic reactions have "early" transition structures (ones more similar to the reactants) [92–94]. The practical implementation of this rule requires a clear definition of the degree of similarity between two different conformations. Usually, this similarity is assessed by describing molecular conformations within classical geometrical terms. In our case, the approach is different. The geometrical notion of molecular structure is replaced by a topological one, defined in terms of *open sets in configuration space* [13]. If molecules are modelled with VDWSs, then a molecular shape corresponds to a domain of configurational space where the topological shape of the VDWS is invariant to geometrical changes within the domain (a shape region). For instance, if there are only three shape regions along a reaction path, then all the nuclear geometries lying

between the reactant geometry and the region where one finds the shape of the transition structure are topologically equivalent in the above sense. For all these geometries, the VDWSs exhibit essentially the same shape. Accordingly, all these geometries represent the "reactant" and they belong to the "reactant domain in configurational space".

The analogous interpretation can be given to the "product domain" and "transition structure domain". In section 5.3, we discuss some examples of application for some simple chemical rearrangements.

5. Comparison between partitionings of configuration space M in terms of potential energy catchment regions and in terms of molecular shape

Some relationships between potential energy and molecular shape can be illustrated within two-dimensional conformational subsets of the configurational space. Molecules exhibiting two internal rotors have been considered as examples in refs. [17] and [96]. Vibrational problems are studies in ref. [22]. In the following, the term "shape" will be used in the context of a given shape descriptor, such as a Van der Waals type: two shapes are the same if their Van der Waals types agree.

Some results for double rotors are illustrative. The examples chosen are catechol (1,2-dihydroxybenzene), resorcinol (1,3-dihydroxybenzene), and hydroquinone (1,4-dihydroxybenzene). The shapes of these systems, undergoing rigid rotations from stationary point geometries, are discussed in detail in ref. [17]. Relaxed geometries, allowing the nonrigidity in the torsion to be taken into account, are analyzed in ref. [96].

The subspace of internal coordinates considered is defined as follows. In order to reduce the size of the problem, the angles and bond lengths relating to the carbon and hydrogen atoms of the benzene ring are kept constant at their experimental values for the benzene molecule. The potential energy has been minimized over a subspace of eight internal coordinates for every pair of torsion angles. These coordinates consist of two O–H distances, two C–O distances, two COH bond angles, and two CCO bond angles. This subset of coordinates involves those on which the torsional, nonrigidity effects are the greatest. Within this subset, the potential energy is minimized at the STO-3G ab initio level, using the standard Gaussian 86 program [97]. This approximation level is sufficient to obtain reliable geometries and the essential topological features of the potential energy surfaces for the above two-dimensional torsional problems.

The molecular surface associated to each nuclear geometry is modelled by a fused-sphere Van der Waals surface (VDWS). Below, we compare the catchment regions with the shape regions S_i, where the shape of the VDWS remains invariant. The number and type of shape regions S_i will depend on the molecule considered.

Let us first consider the case of hydroquinone. It is the simplest of the three systems, since the shape of the molecular surface and the potential energy function

exhibit the fewest features. This is due to the fact that the two OH groups are the most distant from each other.

The potential energy map has four different minima, four maxima, and eight saddle points in the unit cell. The pattern of the contour map has D_{2h} symmetry, only slightly distorted from D_{4h} symmetry.

As a comparison, the shape invariance region map has strict D_{4h} symmetry. Figure 1 compares molecular shape and potential energy [96]. Various regions in the diagram for molecular shape represent shape regions. Various letters indicate distinct shape descriptors, such as those discussed in section 4.

The molecular shape, as defined by the given invariants, is "blind" to the small distortion from (and the loss of) the D_{4h} symmetry in the potential energy. Notice that a distinct shape can be associated to every type of critical point: shape "A" (see table 1(a)) to the maxima, shape "B" to the minima, and shape "C" to the

Table 1

Shape invariance region classification for the torsional conformational subset of structural isomers of dihydroxybenzene. Shape classification is given only for regions whose shape coincides with that of a critical point.

1(a) *Hydroquinone (1,4-dihydroxybenzene)*

Shape region	ϕ	χ
A	{4,10}	{−2,(1,1,1,1)}
B	{4,0,0,12}	{−2,2,2,(1,1,1,1)}
C	{4,5,0,6}	{−2,(1,1),2,(1,1,1)}

1(b) *Catechol (1,2-dihydroxybenzene)*

Shape region	ϕ	χ
A	{4,10}	{−2,(1,1,1,1)}
B	{4,2,0,6,0,0,0,2}	{−2,(1,1,1),2,(1,1,1,−1),2,2,2,1}
C	{4,4,0,2,2,2,0,1}	{−2,(1,1,1,0),2,1,0,0,2,1}
D	{4,2,0,10}	{−2,(1,1,1),2,(2,2,2)}
E	{4,4,2,4,0,2}	{−2,(1,1,1,1,1),0,0,2,1}
F	{4,5,0,3,0,1,0,1}	{−2,(1,1,1,0),2,(1,1),2,1,2,1}

saddle points. Observe that two, apparently different surfaces, for instance, those of the two planar minima, are classified as *having the same topological shape*, as defined by the given descriptors.

The similarities between the shape invariance maps and the potential energy contour maps allows one to carry out the analysis from a different point of view. Since the pattern of shape domains of the VDWS mimics very closely that of the catchment regions of the potential energy function, the latter can be thought of as

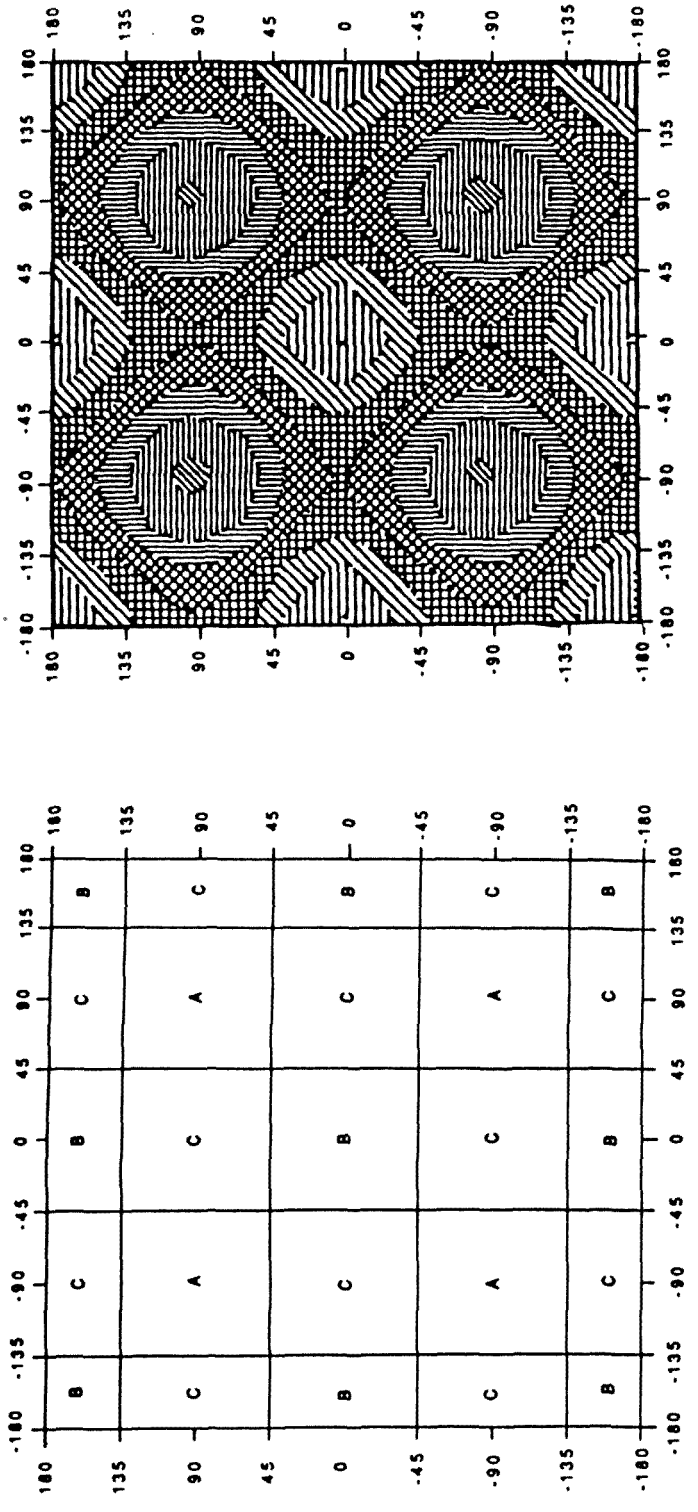

Fig. 1. The potential energy and shape invariance region maps for the hydroquinone molecule (1,4-dihydroxybenzene). Energy given in hartrees, angles given in degrees. Boundaries indicated have an uncertainty of 15°.

reflecting essentially hard-sphere type features. In this sense, the relation between molecular shape (as described by the fused-sphere SGM) and potential energy gives one a criterion to establish the importance (in some cases dominance) of the steric repulsive character in the energy contribution.

For the second isomer, resorcinol, the shape and potential energy maps exhibit new features since the two hydroxylic groups are closer to each other. The overall pattern of the potential energy map is similar to the one for hydroquinone (the same number of critical points occur) [96], and is not displayed here. However, the deviation from the D_{4h} symmetry is now more pronounced than in the case of hydroquinone. The distortion from the symmetry D_{4h} in the potential energy contour map is accompanied by a similar distortion in the shape invariance map. It is still possible to associate a characteristic shape to every type of critical point. Moreover, catchment regions (for minima) of different sizes correspond to molecular surfaces with different shapes. Nevertheless, not every shape invariance region can be associated with a critical point. In other words, the surface exhibits some shape characteristics which do not appear to correlate directly with the major features of the potential.

For catechol, one has the strongest interaction between hydroxylic groups during the internal rotations. Accordingly, during torsional motion this molecule exhibits very different features, both in its molecular shape and potential energy function. Figure 2 shows the results for the shape map (left) and the potential energy contour map (right). Table 1(b) summarizes the results for the shape descriptors ϕ and χ characterizing the more relevant shape regions. Notice that the number of critical points has changed. The energy contour map has three minima instead of four. The shape invariance region map shows features consistent with the potential contour map, as well as some differences. Firstly, one notices that all maxima have associated molecular surfaces with the same shape (shape "A"), although the boundaries of shape regions are different for different maxima.

Regarding the saddle points, all those that are of different energy according to the potential are also classified into different shape regions (shapes "F", "E", and "D").

Although it is possible to classify the critical points according to the shapes of their corresponding molecular surfaces, there are numerous shape regions not associated with any of the main features of the potential energy function. As suggested by the case of catechol, the number of shape regions seems to be greater in the neighborhood of saddle points.

The examples provided some clues to the understanding of the relationships between changes in molecular shape and changes in potential energy induced by conformational reorderings. As observed, the pattern of distribution of shape invariance regions follows closely the topological pattern of potential energy features. That is, different types of critical points are associated with molecular surfaces which have different shapes. Moreover, the extent and shape of the catchment regions are often comparable to the extent and shape of an associated shape invariance region. However, the topological molecular shape can remain unaffected by the occurrence of certain

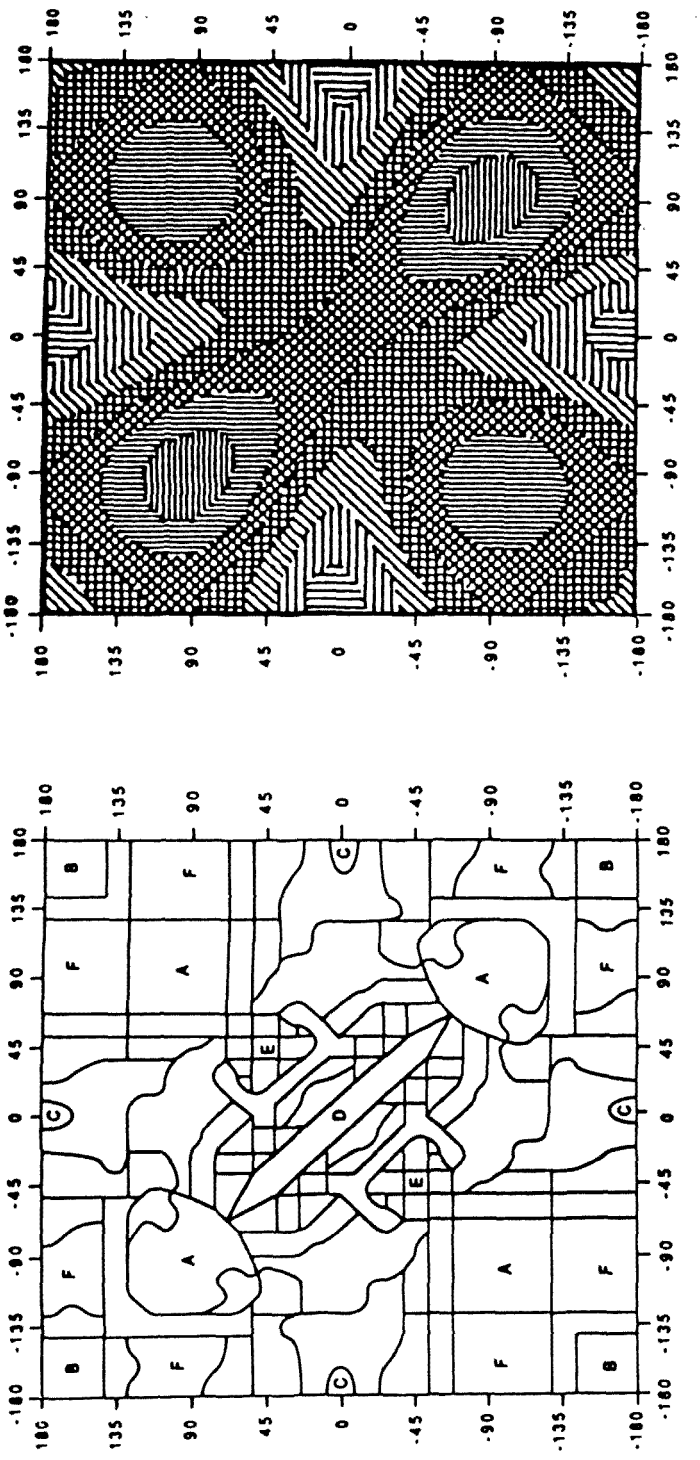

Fig. 2. The potential energy and shape invariance region maps for the catechol molecule (1,2-dihydroxybenzene). Energy given in hartrees, angles given in degrees. Boundaries indicated have an uncertainty of 7°.

features of the potential. For example, critical points of the same type, but with different geometries, can have associated molecular surfaces of equivalent shapes. On the other hand, molecular surfaces can exhibit shape changes that do not correspond to any of the main features of the potential. These shape changes can be physically meaningful, since they may correspond to major rearrangements of atoms occurring along a path of conformational change in which the potential energy varies monotonously.

Summarizing the above, chemical processes are dependent not only on the change in energy content, but also on the shape of electron density generated by the spatial arrangement of atomic nuclei within a molecular system. Quantum mechanics provides an accurate method for determining how the energy changes in a molecule, but provides only indirect information about molecular shape, since the concept of molecular shape is in fact classically motivated [1,2,98]. In this sense, molecular shape maps and potential energy maps contain essential information that cannot be fully deduced from one another.

5.2. ONE-DIMENSIONAL TORSIONAL PROBLEMS AND MOLECULAR SHAPE. DILATATIONS OF MOLECULAR SURFACES

The location of the boundaries of VDWS shape regions varies with the choice of atomic radii. If one allows the radii to vary within some physically meaningful ranges, then the boundaries will become boundary ranges between regions. These boundary ranges represent the fuzzy nature of molecular species and molecular surfaces [1,2,98].

One can use various approaches to describe such fuzziness [13]. One consists of computing the molecular shape descriptors for the different choices of atomic radii available in the literature. This approach is illustrated in refs. [20] and [21], when following the changes in molecular shape along reaction paths.

On the other hand, one can study systematically the changes in shape when modifying the atomic radii continuously. Consider a common scaling factor f affecting all atomic radii: $r_i(f) = f r_i(1)$, where $r_i(1)$ can represent, for example, the standard radii quoted in ref. [99]. Figure 3 shows some results illustrating this type of analysis. At the top, fig. 3 displays the changes in shape for the rotational conformers of ethane, studied as a function of the scaling factor f. Different numbers indicate distinct shape regions, characterized by different sets of shape descriptors φ and χ as listed in table 2. On the right of the figure, we indicate the radii on which the scaling is performed. The diagram at the bottom provides a similar description for the internal rotation in methanol. In both cases, geometries have been computed at the ab initio level with the standard 3-21G basis set. Technical details on the study of these and other one-dimensional torsional systems are given in ref. [20].

Figure 4 compares the rotational potential wells for ethane and methanol, both in terms of energy and molecular shape. Dotted lines indicate the boundaries of different shape regions found along the internal torsional transformation. These

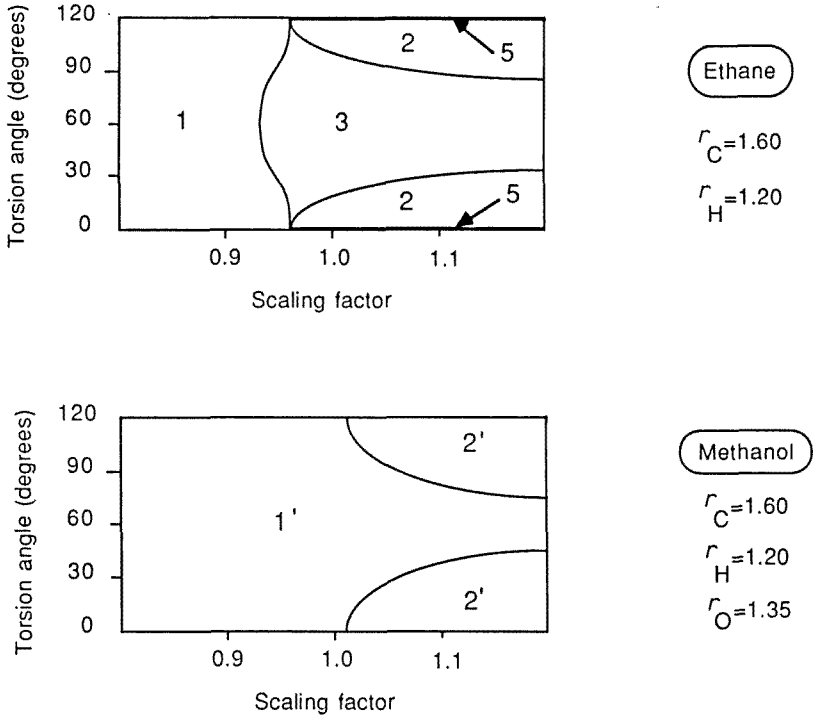

Fig. 3. Shape region maps for torsional problems of threefold symmetry, considering isotropic scaling of atomic radii from the most convoluted VDWS. (See table 2 regarding the notation used for the shape regions.)

Table 2

Shape classification for the VDWSs of some rotational problems of threefold symmetry (cf. figs. 3 and 4).

(1) *Ethane*	ϕ	χ
1	{8}	∅
2	{0,0,6,0,0,0,0,0,2}	{2,2,−1,2,2,2,2,2,(1,1,1)}
3	{0,6,0,0,0,0,0,0,0,0,0,2}	{2,−4,2,2,2,2,2,2,2,2,2,(1,1,1,1,1,1)}
4	{0,0,0,6,0,2}	{2,2,2,(1,1),2,0}
5	{0,6,0,0,0,2}	{2,−1,2,2,2,(1,1,1)}

(2) *Methanol*	ϕ	χ
1′	{3,3}	{−1,(1,1,1)}
2′	{2,2,0,2}	{0,0,2,(1,1,1,1)}

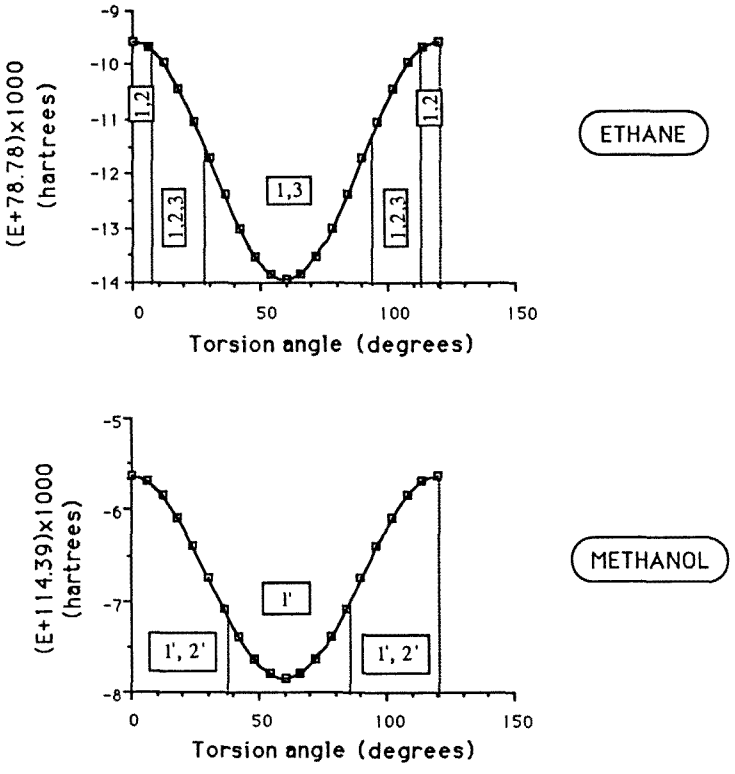

Fig. 4. Comparison of shape invariance regions of torsional angles with chemical species defined in terms of the potential energy function (rotamers). (Dilatations of 10% from the most convoluted surface are considered. See table 2 regarding the notation used for the shape regions.)

boundaries were estimated by allowing ±10% changes of the Van der Waals radii around the reference values. Observe that in both cases it is possible to associate definite and distinct shapes to the conformers corresponding to the critical points of the potential energy function. In the particular case of ethane there appears a third, intermediate shape between those of the staggered and eclipsed conformations.

In all cases, the above approach provides an explicit measure of the degree of similarity among molecular surfaces encountered along a conformational motion. The fuzziness in the definition of the molecular surface can be expressed quantitatively by the sizes of regions where more than one molecular shape exists. An alternative approach to quantifying this fuzziness is given in ref. [100].

Other one-dimensional torsional problems are analyzed in ref. [20]. From this study, a one-way assignment of critical points of the potential energy to shape regions emerges. The assignment is one way since the shape regions can outnumber the catchment regions of the potential energy function. One can characterize chemical

species by specific domains in configuration space with defined molecular shapes in terms of given shape descriptors. However, there will in general be other domains with characteristic shape with no direct correspondence to catchment regions. Nevertheless, as said before, the occurrence of these additional shape regions can be physically meaningful. Changes in the shape of a molecular surface may not be apparent when following potential energy changes, since the latter can vary monotonously along a conformational path. This information, not seen when studying energy, becomes explicit if one uses shape descriptors.

5.3. MOLECULAR SHAPE CHANGES ALONG REACTION PATHS

The procedure discussed in the previous section can be employed to describe the interrelation between energy and molecular shape along an arbitrary reaction path.

The isomerization reaction HNC→HCN provides an interesting example to analyze the structural changes along a reaction path. This problem has been studied in ref. [21] using the results of a classic paper by Pearson et al. [101], where the minimum energy path was computed at a large-scale CI level.

As reaction coordinate, we use the arc length of the path $P(t)$ represented in a mass-weighed Cartesian system of coordinates. In this case, the arc length $s(t)$ is given to a good approximation by:

$$s(t) \approx \int_{x'_0(\mathrm{H})}^{x'_t(\mathrm{H})} \left[1 + \left(\frac{\mathrm{d}\, y'_p(\mathrm{H})}{\mathrm{d}\, x'_p(\mathrm{H})} \right)^2 \right]^{1/2} \mathrm{d}\, x'_p(\mathrm{H}), \tag{18}$$

where $x'_p(\mathrm{H})$ and $y'_p(\mathrm{H})$ represent two mass-weighed coordinates of the H atom, that is, a Cartesian coordinate $x(\mathrm{H})$ or $y(\mathrm{H})$ multiplied by the square root of the mass of hydrogen. (Note that if the rearrangement affects only a single nucleus, then the mass-weighing is not essential.) The subindex attached to the coordinates represents the progress along the reaction path as measured by parameter t. For example, $x'_0(\mathrm{H})$ corresponds to the mass-weighed x coordinate for the hydrogen atom in the starting configuration, whereas $x'_t(\mathrm{H})$ is the x coordinate at position $P(t)$ along the reaction path.

Figure 5 shows the reaction barrier for the reaction as a function of the arc length s. The reaction HNC→HCN is exothermic. Nevertheless, the barrier is *late* for HNC, *contrary* to the Hammond postulate. The HNC geometry lies 2.5 units of arc length away from the transition structure, while the HCN geometry lies at only 2.0 units from it.

Using the shape characterization methods discussed previously, only two shape transitions are found along the reaction path. The essential shape features of the VDWSs for reactant and product are the same. The transition structure corresponds to a molecular surface with a different topological shape, one where the three

atomic spheres interpenetrate. (The molecular surface for the transition structure is homeomorphic to a 2-sphere and not to a 2-torus.)

On can easily compute the limit geometries along the reaction path at which "shape transitions" $\tau_R \rightarrow \tau_T$ and $\tau_T \rightarrow \tau_R$ occur, where "τ" represents the shape descriptor chosen. The locations in general change with the sets of Van der Waals atomic radii chosen. One can compute these geometries for all atomic radii for C, N, and H. After determining the geometries, the corresponding values of arc length on the reaction path can be evaluated using eq. (18) as described above. The results are shown in fig. 5. The shaded regions in the diagram show the uncertainty in the

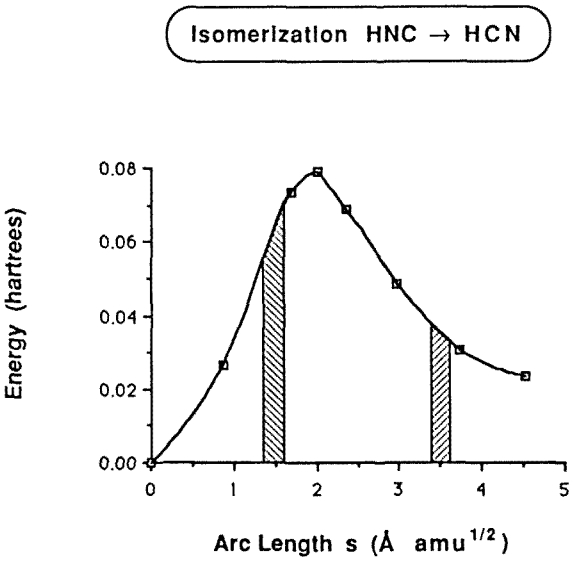

Fig. 5. Reaction barrier for the HCN isomerization with the arc length along the reaction path (eq. (5)) as reaction coordinate. (The electronic energy is measured relative to HCN. The abscissa varies from HCN to HNC; masses are measured in a.m.u. in order to compute the arc length in mass-weighed coordinates. Shaded regions represent the uncertainty in the boundaries where the change in shape for the molecular surface occurs. This uncertainty is due to the range of possible choices of VDW radii for each atom.)

location of the shape changes $\tau_R \rightarrow \tau_T$ and $\tau_T \rightarrow \tau_R$ due to the uncertainty in the values chosen for the radii. These regions represent a formal "boundary range" among the shape regimes dominated by the shape characteristics of the reactant, product, and transition structure. These boundary ranges are equivalent to those found for conformational problems in the previous section, upon considering dilatations of the molecular surface.

Figure 5 shows that the boundary between the reactant and transition structure regions lies only at approximately 1.0 units of arc length away from the reactant's formal geometry. On the other hand, the boundary for the product and transition structure region is about 1.5 units of arc length away from the product's formal geometry. In other words, *the reactant (HNC) molecular surface may attain the topological shape of the transition structure molecular surface by a distortion of nuclear geometry smaller than that required for the product (HCN) molecular surface.* It is noteworthy that this result is in agreement with the Hammond postulate, if the notion of molecular structure is understood as a topological concept, defined by the shapes of the Van der Waals surfaces.

The topological definition of molecular structures in terms of 3D molecular shape descriptors leads to new insights. The present results provide another point of view for the studies of similarities: the relevant domains of the nuclear configurations are determined by the invariance of the topological shape of the molecular envelope. The reinterpretation of the Hammond postulate according to similarity defined by shape descriptors may reclassify some reactions showing a formal violation according to the standard formulation.

The studies on hydrogen-shift reactions, other than the type [1,2], are relatively less numerous. As a second illustrative example of the interrelations between electronic potential energy and molecular shape along reaction paths, we discuss a type [1,3] isomerization. The problem is the formal formic acid–formic acid "isomerization" by hydrogen shift between the two oxygen atoms. This problem has recently been studied in detail at various levels of ab initio approximations [102].

The analysis has been performed at two levels. (In ref. [22], we present a more technically detailed discussion.) A first approach has been the construction of a Hartree–Fock (RHF) relaxed cross section of the energy surface and the computation of the minimum energy reaction path. In a second approach, the minimum energy path is recalculated with a full geometry optimization, including configuration interaction within the framework of second-order Møller–Plesset many-body perturbation theory (MP2). In both cases, the 3-21G basis set was employed, using the program Gaussian'86 of Pople and co-workers [97].

The reaction path's arc length (computed in mass-weighed Cartesian coordinates) is considered as the reaction coordinate, in analogy with the case of HCN. The reaction coordinate domain is divided into segments representing the shape domains. Results are shown in fig. 6. A shape transition $A \rightarrow B$ occurs at approximately 0.19 $\text{Å} \cdot \text{amu}^{1/2}$, whereas the change $B \rightarrow C$ occurs at approximately 1.01 $\text{Å} \cdot \text{amu}^{1/2}$, where A, B, and C represent three distinct shape regions according to the Van der Waals shape descriptors. This representation provides a clear recognition of the interrelation between potential energy and molecular shape along the reaction path. In contrast, within the catchment region partitioning of the potential energy surface, no transition is found until the path reaches the transition structure.

In order to analyze the changes in the results introduced by the changes in the level of computation, the minimum energy reaction path was recalculated at the

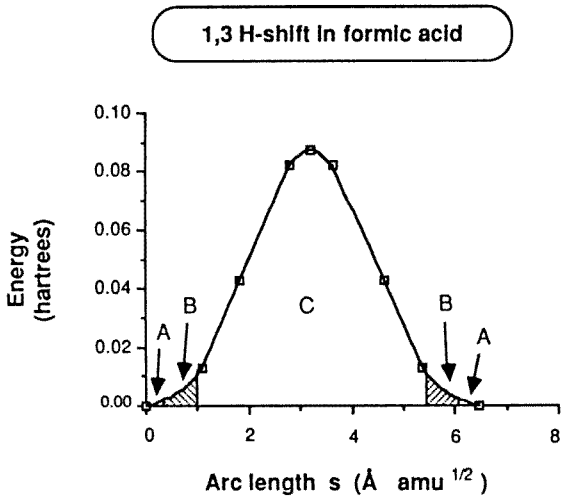

Fig. 6. Reaction barrier for the [1,3] hydrogen-shift rearrangement in formic acid, at SCF 3-21G level. The occurrence of various shape regions is indicated by the letters A, B, and C [22].

MP2 level. No new shapes were found. That is, although the MP2 path deviates in places quite substantially from the RHF path, the deviations are not significant in terms of shape. We may conclude that, despite the differences in energy content, the overall characteristics of the two reaction profiles are quite similar regarding the changes of molecular shape.

The approach discussed can be extended easily to other molecular surfaces. Shape groups, shape graphs, and other shape descriptors of charge densities, as functions of nuclear configurations, are associated with various domains of the configuration space. In the general case, the formal reaction path passes through several of these shape domains of the configurational space, and segments of the path can be characterized by the shape domains to which they belong. The order of occurrence and the relative lengths of these path segments can characterize the shape changes of charge density during the reaction. Nonetheless, Van der Waals surfaces approximate surprisingly well some isodensity surfaces [40,41], and many of the shape changes found and analyzed here are expected to be found also for isodensity surfaces [103].

6. Characterization of foldings in macromolecular models

6.1. FOLDINGS OF MACROMOLECULAR BACKBONE STRUCTURES IN CONFIGURATIONAL SPACE

Let us consider a ribbon-like surface R as our model to describe some of the essential shape features of macromolecules [69–72]. If the set R is a single, noncyclic

ribbon model (RM) that has zero thickness, then R can be chosen so that it is topologically equivalent to a rectangular planar domain and also to a two-dimensional disk. Let $\boldsymbol{r}(t)$ be a parametric space curve, given as follows [73]:

$$\boldsymbol{r}(t) = x(t)\boldsymbol{i} + y(t)\boldsymbol{j} + z(t)\boldsymbol{k}, \qquad 0 \leq t \leq 1, \tag{19}$$

that is located on R, $\boldsymbol{r}(t) \in R$ for all t, along the longitudinal median line of the ribbon. The three unit vectors of an orthogonal Cartesian framework taken as a reference are indicated by the usual symbols $\boldsymbol{i}$, $\boldsymbol{j}$, and $\boldsymbol{k}$. The change in parameter t from 0 to 1 provides an orientation to the space curve, and hence to the ribbon. Here, $\boldsymbol{r}(0)$ corresponds to the "starting" point of the curve (beginning of the ribbon) and $\boldsymbol{r}(1)$ to the "end" point. Functions $x(t)$, $y(t)$, and $z(t)$ in eq. (19) need to be only sectionally continuous. This will be the case, for example, when the ribbon is formed by several disjoint sections. There is an infinite number of curves $\boldsymbol{r}(t)$ that can be traced on the surface R along the longitudinal direction; we shall choose the space curve as the median line of the ribbon. The replacement of a molecular ribbon by an associated space curve (a "molecular space curve") is a simplification that eliminates many structural details. Yet, the space curve retains the essential information needed to describe folding patterns as well as other features of the backbone structure of large chain molecules.

The curve $\boldsymbol{r}(t)$ mimics the features of the molecular backbone. If the two end points are joined then, in general, such an object is a topological knot and, accordingly, it can be studied by means of the branch of topology known as knot theory [82]. The usefulness of knot theory to several chemical applications, for instance, molecular chirality, is well documented (see, for example, refs. [104–113], and others quoted therein). Its relevance to the description of the entanglement of macromolecular chains has also been recognized [74,75]. A knot-theoretical description permits one to recognize the occurrence of certain topological features which remain invariant to conformational motions allowed to the molecule (as long as the chains are not broken and no self-crossing occurs). Among these invariants one can mention the linking number [76] and the writhing and twisting numbers [76–79]. These three numbers may be used for the characterization of a ribbon model.

However, the above description may disregard important characteristics of the macromolecular folding. Overcrossings of side chains, changes in tertiary structure in proteins, the opening of protein cavities all represent relevant features for understanding protein dynamics and reactivity (e.g., refs. [115–117]). Yet, these features are not represented in such a description simply because they do not lead to a change in the knot type or fundamental group [82]. Moreover, in an overwhelming number of cases, the protein backbone structure, as described by molecular ribbons, tubes or space curves, leads to simple loops that are not knotted, that is, *unknots* [82]. In order to derive a more informative description, a transformation could be introduced on the space curve, such that it may assign a knotted structure to the original unknotted object (see next section).

6.2. TWO APPROACHES TO CHARACTERIZATION: GRAPH-THEORETICAL AND KNOT-THEORETICAL ANALYSES

Let $\boldsymbol{r}(t)$, $0 \leq t \leq 1$, be our space curve, associated with the backbone of a chain molecule, as discussed in the previous section. Let us further assume that $\boldsymbol{r}(t)$ is confined to a finite region of the 3-space.

In order to characterize some shape features of the curve, one can introduce a graph-theoretical characterization of a number of its projections. This description provides a discrete characterization of the curve which is simple and appropriate for computer manipulation. The projections of the space curve $\boldsymbol{r}(t)$ are chosen according to the axes of a preferential coordinate framework. This framework will be taken to be the one given by the three orthogonal axes of inertia. The choice of the three axes, indicated by the triplet (Q_1, Q_2, Q_3), guarantees that the shape features will not depend on translations and rigid rotations. $P(Q_i)\boldsymbol{r}(t)$ will indicate the projection of the curve $\boldsymbol{r}(t)$ onto a plane $Q_i = Q_i$, where Q_i is a fixed coordinate value along the axis Q_i. The result of this operation is a plane curve, denoted as $\boldsymbol{q}_i(t)$:

$$\boldsymbol{q}_i(t) = P(Q_i)\boldsymbol{r}(t), \qquad 0 \leq t \leq 1. \tag{20}$$

The projections appear as plane curves exhibiting a number of overcrossings; these overcrossings are the consequence of observing the space curve curling over onto itself from a certain direction in space. The occurrence of these overcrossings characterizes the plane curves $\boldsymbol{q}_i(t)$, $i = 1, 2, 3$, and, in turn, the space curve $\boldsymbol{r}(t)$.

Let us associate a graph g_i to each curve $\boldsymbol{q}_i(t)$, described here in terms of intuitive concepts. The vertices of these graphs are the curve's overcrossings (crossovers), and the edges are the segments of the curve connecting crossovers. Note that these segments can connect two different crossovers, or a crossover with itself. Segments of the curve not providing connections beween vertices will be dropped from the graph. From these intuitive notions, the formal definition of the graph g_i can be given:

(i) *Vertices of the graph*: A vertex is a maximum connected subset of points on the planar projection where two or more segments of the space curve are projected onto one another as viewed from the given preferential direction in 3-space. Notice that crossovers can occur not only as isolated points, but also entire parallel sections of the projected curve can appear to cover each other. The vertices are collected in an ordered set $V(g_i)$:

$$V(g_i) = (v_{i1}, v_{i2}, v_{i3}, \ldots). \tag{21}$$

The ordering is established from the orientation along the original space curve. The vertices are numbered according to their occurrence when moving along the curve.

(ii) *Edges of the graph*: If two vertices of the graph are connected by a section of the planar projection of the space curve containing no other vertex, then this

section will be regarded as an edge connecting them in the graph. In most cases, multigraphs will be found (i.e., more than one edge connects two vertices), and pseudographs may also occur (containing an edge starting and ending at the same vertex). The set of edges of a graph g_i will be indicated by $E(g_i)$. According to our construction, a segment of the plane curve not starting from or not ending at a vertex will not contribute an edge to g_i, that is, in the graph the "end segments" of the chain beyond the terminal crossing are disregarded.

The three graphs g_1, g_2, and g_3 associated with the space curve $\boldsymbol{r}(t)$ obtained from the ribbon R provide a concise description of some of its shape features. The basic information defining the graph is contained in its adjacency matrix, which can be easily analyzed. One can introduce additional information within the graph. For example, one can associate with each vertex a crossing index, characterizing the type of overcrossing in the space curve which defines the vertex in the graph. If v_{ij} indicates the jth vertex of the graph g_i (numbered according to the order of occurrence along the curve), its corresponding crossing index C_j is defined as follows: $C_j = 1$, if the vertex comes from a *right-handed crossover*, $C_j = -1$, if it comes from a *left-handed crossover* [82]. This complementary information, as vertex labels for a graph with n vertices, is stored in the vector $\boldsymbol{C}(g_i)$:

$$\boldsymbol{C}(g_i) = (C_1, C_2, \ldots, C_n). \tag{22}$$

This procedure can be followed as long as all the crossings are regular. Several degenerate crossings can be expected. For instance, more than two sections of the curve can cross over the same point, a section of the curve can osculate another at a single point, two or more sections of the curve can become superimposed completely (i.e., there are infinitely many overcrossing points). All these cases can be addressed by choosing values of the crossover index C_j different from ± 1 that allows one to distinguish all possible degenerate cases.

In one follows the change of a ribbon along a conformational path (for example, a continuous folding of the protein backbone), both the graph and the set of crossing indices change. However, this change will be *discrete*: only for certain values of the parameters defining the conformational rearrangement will the folding pattern exhibit essential changes, as reflected by the projections and changes in the graph. Consider, for example, a closed space curve, one of whose projections is followed during a folding. This case is schematically depicted in fig. 7. It may correspond to observing rearrangements in a large molecular cycle or loop. The right-hand side of the diagram shows the changes in $\boldsymbol{C}(g_i)$, which occur only at specific conformations.

Summarizing this approach, in conformational motions of large macromolecular chains their shapes are regarded equivalent if and only if their topological shape features are preserved as described by the projected, vertex-labelled plane graphs.

Consider as an illustrative example a small irregular protein, the λ-Cro Repressor protein, whose ribbon model is given in ref. [69]. The left-hand side of fig. 8 shows

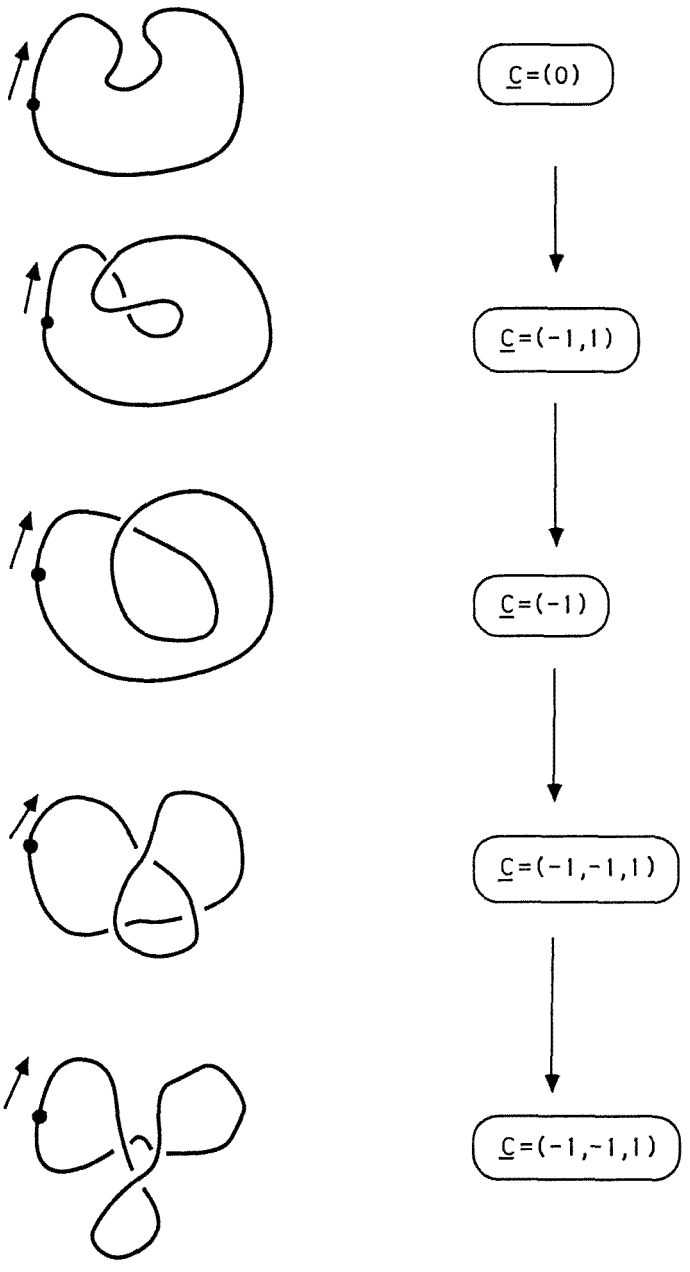

Fig. 7. Characterization of foldings in a closed space curve by means of the vectors of crossing indices (eq. (22)).

a view of the molecular skeleton, in terms of space curve, from three orthogonal directions of observation. The curve corresponds to the model with structureless helices [69,70]. This simplified molecular space curve shows the interrelations

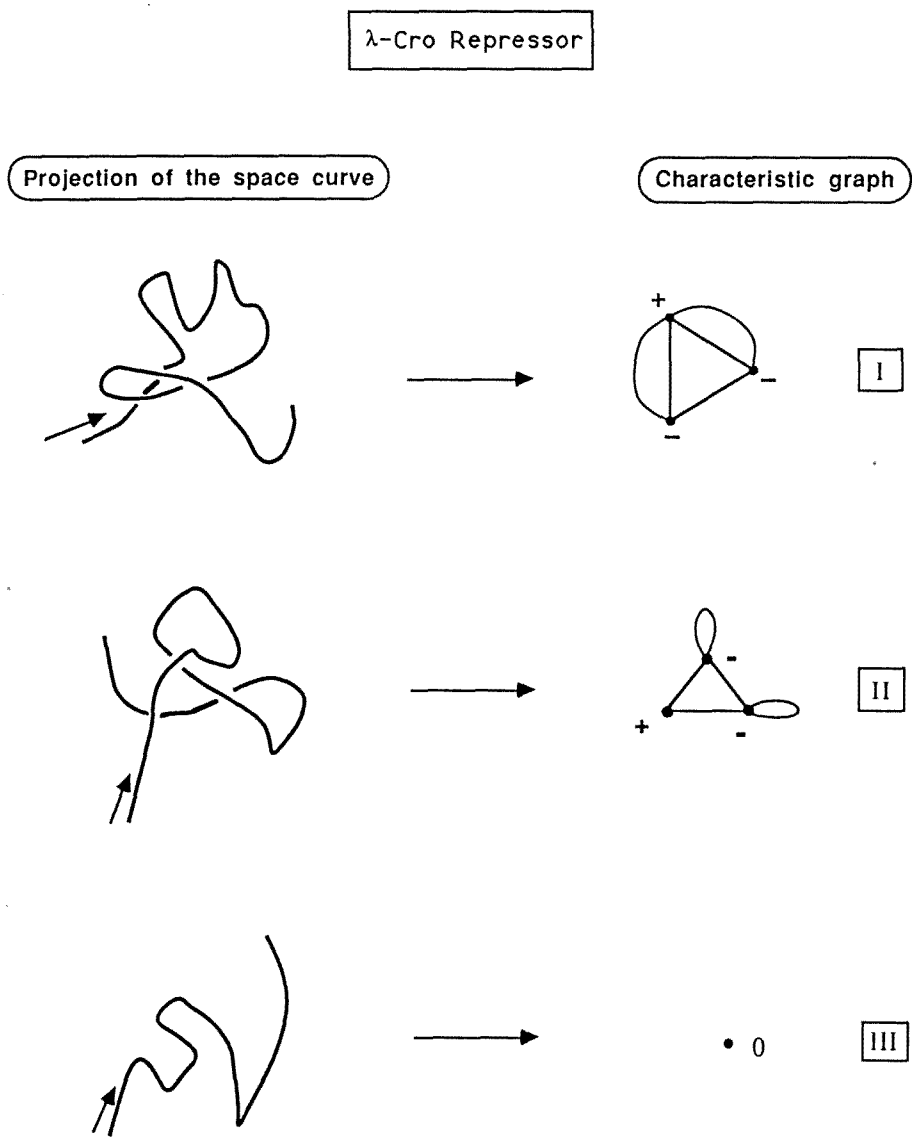

Fig. 8. Graph characterization of three orthogonal projections of the λ-Cro repressor protein.

among the elements of the secondary structure (helices, β-strands, and loops). The right-hand side of fig. 8 shows the corresponding graphs, with crossing indices marked on their vertices.

As mentioned above, knot theory provides an alternative approach to describe conformations of macromolecules and their changes along folding paths. A mathematical knot K is a closed space curve in 3D, where the "degree and type of knottedness"

can be charactized by various projections of the curve onto planes [82]. A *regular projection* is one that corresponds to no degenerate crossings, that is, at each point at most two segments are projected on one another. If the knot is represented by a string, then the identity of the knot is not affected by changing the shape of the string, and all motions of the string are allowed as long as it is not cut or rejoined anywhere. The various allowed 3D arrangements of the string are called *placements*. It is possible to select placements so that the number of crossings of the string is minimized in a regular projection; the *crossing number* is the number of crossings obtained in such a case. If the string is given an orientation, then each nondegenerate crossing can be characterized by its handedness.

It is possible to assign polynomials to each knot, based on the handedness of crossings in any regular projection of any placement of the knot. These polynomials have a remarkable property: they are invariant to the choice of placement of the knot. That is, for a given knot, one obtains the *same* polynomial, independent of how complicated is the actual arrangement of the string, and by how much the actual number of crossings exceeds the crossing number. These polynomials are topological invariants of the knots and can be used for their characterization. Among these polynomials, the Jones polynomial $V_K(t)$ of a knot K is of major interest [105,106], since it can serve, among other roles, as a tool for detecting chirality of knots. A knot is topologically chiral if no rearrangement of the string can bring the knot into superposition with its mirror image.

Our interest in knot-theoretical representations stems from the fact that these polynomials provide a nonvisual, algebraic shape characterization of curves in 3D space; hence they are of relevance in the characterization of space curves representing the backbone structure of chain molecules.

The original space curve of the median line of the ribbon is not in general a knot, since the two endpoints of the median line are usually not joined. However, *for the given projection* we may convert the space curve of the median into a knot K_a by the following steps:

(i) Attach to each endpoint of the space curve a straight line segment, perpendicular to the viewing plane, pointing away from the viewer, and reaching a plane, parallel with the viewing plane, far removed from the ribbon.

(ii) Join the far ends of these line segments by another straight line segment, parallel with the viewing plane.

This procedure converts the median curve into a closed curve that is in general a knot, denoted by K_a. In the strict sense, a simple loop is not knotted; it is often called the "unknot". For the sake of simplicity, we shall refer to it as a formal member of the family of knots. We shall analyze the resulting object K_a on two levels:

(a) describe the object itself, regarded as a knot K_a in 3D space, by taking the corresponding Jones polynomial $V_{K_a}(t)$, and

(b) consider the projection of K_a to the original viewing plane, and find various (possibly all) knots K_b that are compatible with the projection. A knot K_b may be selected that preserves the most crossings. The Jones polynomial $V_{K_b}(t)$ of the knot K_b is used to characterize the projection.

The construction of the Jones polynomial $V_{K_a}(t)$ in level (a) of the characterization of the ribbon model follows the standard procedure. The mathematical approach is described in detail in refs. [105] and [106]. A detailed, pictorial description has been given in the chemical literature [113].

One important question arises: which knots are compatible with a given set of projections? This partial reconstruction problem will be illustrated for the median line of the simplified tertiary structure of the λ-Cro Repressor protein, used previously (fig. 8, projection I, top). Other examples are discussed in greater detail in the literature [80,81].

We assume that the extension lines of steps (i) and (ii) for the conversion of the median curve into the knot K_a add at most nondegenerate new crossings to the projection. The latter condition can always be fulfilled by an infinitesimal distortion of the ribbon model. (In the case of the example, no new crossing occurs.) All n crossings of the projection can be characterized by the numbers $C_j = +1$ or -1, collected into a vector $\boldsymbol{C}$ as in eq. (17).

All possible knots with the same 2D projection (with crossing information suppressed) and with arbitrarily chosen handedness for the crossings can be reconstructed by suitably modifying some or all n of the C_j numbers. By taking an n-dimensional switching vector

$$\boldsymbol{v} = (v_1, v_2, \ldots, v_n), \tag{23}$$

with elements

$$v_j = +1, \text{ or } -1, \tag{24}$$

a new vector $\boldsymbol{C}^{\boldsymbol{v}}$ is generated from the reference vector $\boldsymbol{C}$ by taking

$$\boldsymbol{C}^{\boldsymbol{v}} = (C^{v_1}, C^{v_2}, \ldots, C^{v_n}) \tag{25}$$

with elements

$$C^{v_j} = v_j C_j. \tag{26}$$

If crossing information for a reference projection is not available, then all elements of the reference vector $\boldsymbol{C}$ may be chosen as unity. By taking all the 2^n possible n-dimensional vectors $\boldsymbol{v}$ of form (23), the crossing vectors $\boldsymbol{C}^{\boldsymbol{v}}$ of *all possible knots (and links) compatible with the given 2D projection (with crossing information suppressed) will be generated.* The family of knots obtained is denoted by $\{K_b\}$, and the corresponding family of Jones polynomials is denoted by $\{V_{K_b}(t)\}$. One may take the family of all these Jones polynomials $V_{K_b}(t)$ for characterization.

The supersecondary structure of our example protein is indicated at the top of fig. 8, where the α-helices have been replaced by their axes. The projection of the space curve exhibits only three crossovers. The reference vector $\boldsymbol{C}$ of reference projection C is the actual crossing vector $\boldsymbol{C} = (-1, 1, -1)$ of the reference knot K. For this choice of $\boldsymbol{C}$, the vector v of reference knot K is $v = (1, 1, 1)$. In this case, the knot K is the unknot [82].

Table 3

Knot-theoretical characterization of a projection of the simplified ribbon model for the λ-Cro Repressor protein. (The projection of the molecular space curve exhibits three overcrossings.)

Switching vector	Knot type	Jones polynomial
(1,1,1)	0_1	1
(−1,1,1)	0_1	1
(1,−1,1)	3_1	$-t^4 + t^3 + t$
(1,1,−1)	0_1	1
(−1,−1,1)	0_1	1
(−1,1,−1)	3_1^*	$-t^{-4} + t^{-3} + t^{-1}$
(1,−1,−1)	0_1	1
(−1,−1,−1)	0_1	1

In table 3, we present the results for all knot types that are compatible with the reference projection C and their Jones polynomials. The switching vectors v, given with respect to reference vector $\boldsymbol{C} = (-1, 1, -1)$, are also specified. The most complicated knots occurring are the left- and right-handed trefoil knots (3_1 and 3_1^*, respectively). Following the standard procedure for knot pairs K and K^* that are mirror images [82], the relation

$$V_{K^*}(t) = V_K(1/t) \tag{27}$$

applies, and the Jones polynomials

$$V_{3_1}(t) = -t^4 + t^3 + t, \tag{28}$$

$$V_{3_1^*}(t) = V_{3_1}(1/t) \tag{29}$$

are obtained. These polynomials provide a concise characterization of the given projection of the backbone of the protein tertiary structure as well as a tool for the recognition of chirality properties, using eq. (27). This description can be applied to characterize shape changes along a folding path.

6.3. CHARACTERIZATION OF FOLDINGS BY MAPPING TO SPHERES: A PROJECTION-INDEPENDENT DESCRIPTION OF MACROMOLECULES

The methodology described in section 6.2 requires the definition of three preferential directions from where projections are performed. Although we have chosen the axes of inertia, other choices are also possible; ultimately, the choice of these directions is arbitrary. In this section, we describe an alternative approach that overcomes this arbitrariness by introducing a new type of projections.

Let $\boldsymbol{r}(t)$ be the parametric representation of a bounded molecular space curve C, and let $\boldsymbol{r}_0$ be the centre-of-mass of the corresponding macromolecule. Point $\boldsymbol{r}_0$ almost never falls on the curve. We can define a spherical domain B, centered about $\boldsymbol{r}_0$ and with a radius R, chosen so that B contains the entire space curve C. Let S be the surface of this sphere:

$$S = \{\boldsymbol{r}' \in \mathbb{R}^3 : \|\boldsymbol{r}' - \boldsymbol{r}_0\| = R\}, \tag{30}$$

where $\|\boldsymbol{r} - \boldsymbol{r}_0\| \leq R$, for all $\boldsymbol{r} \in C$.

One can project any point of the space curve to the sphere S by using the straight line connecting such a point with the centre. A point projected onto S will be indicated as $\boldsymbol{r}_S(t)$. The set of points $\{\boldsymbol{r}_S(t)\}$ defines a curve on the sphere. It can have a number of crossovers. The use of this projected curve for characterization of the original $\boldsymbol{r}(t)$ would be akin to some other methods based on mapping of molecular surfaces onto spheres [118,119]. The projected $\boldsymbol{r}_S(t)$ curve can be characterized by the same techniques applicable for any single planar projection of section 6.2.

In an alternative characterization, the points on the spheres are used to generate all possible viewing directions, and to each such point a graph or a family of knots is assigned. In order to characterize the curve $\boldsymbol{r}(t)$, one can use the sphere S as follows. Consider an arbitrary point $\boldsymbol{r}'$ on S as a viewing point for the space curve $\boldsymbol{r}(t)$. From this viewing point, a projection is defined as one to a plane perpendicular to the $\boldsymbol{r}_0 - \boldsymbol{r}'$ vector (tangent plane at $\boldsymbol{r}'$). This projection can be characterized by graph-theoretical or knot-theoretical methods as described above. Let us indicate with $s(\boldsymbol{r}')$ the "shape" of the curve as viewed from $\boldsymbol{r}'$, using some shape descriptor (say, the Jones polynomials for the derived knots, as in section 6.2). This shape analysis can be applied to every point $\boldsymbol{r}'$ on S.

The shape, as defined by the given shape descriptor, may be invariant to most small changes of the viewing point $\boldsymbol{r}'$. As a matter of fact, the sphere S will have only a *finite* number of shape domains. This is schematically represented in fig. 9. On the left, an arbitrary, bounded space curve is shown, surrounded by the sphere S. On the right, one finds the resulting subdivision of the spherical surface into shape regions. Each of the regions is characterized by a different knot description of the curve C. In the particular case depicted in fig. 9, the curve does not exhibit many entanglements, and the characterization requires only the unknot and the trefoil knot.

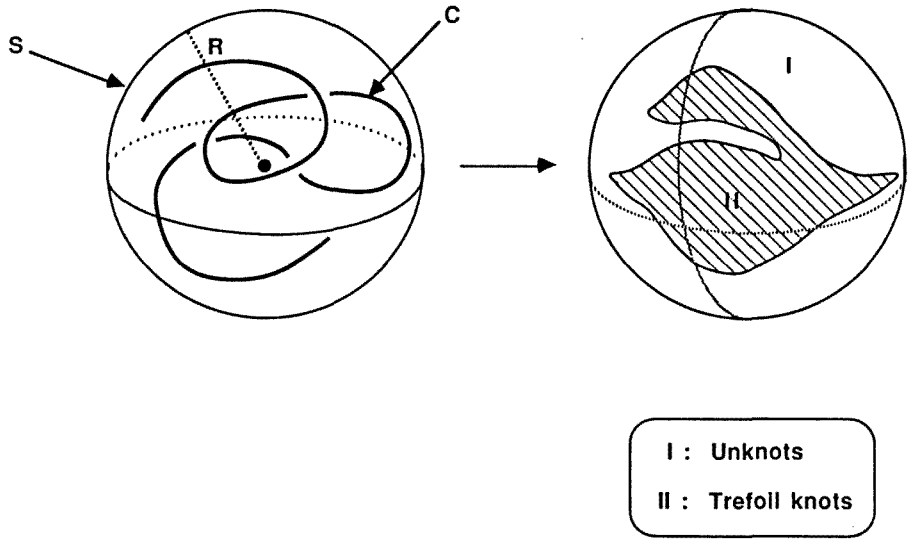

Fig. 9. Direction-independent characterization of a space curve C. The left-hand side shows the sphere S of radius R enclosing the curve C; the centre of the sphere is the centre-of-mass of C. The right-hand side shows the characterization of the curve, in terms of shape regions mapped on the sphere S. The types of derived knots found for the projected curve at different points on S are indicated (see section 6).

The distribution of shape regions on the sphere S enclosing the molecular curve C provides a detailed description of its shape. This approach avoids choosing an arbitrary projection since all the possible projection directions are taken into account.

7. Conclusions and future directions of work

In this review, we have discussed some recent developments in the study of the interrelation between configurational rearrangements and the corresponding changes in potential energy and molecular shape.

Potential energy is a well-defined concept in quantum mechanics. As a result, the potential energy catchment regions of a given electronic state provide a well-defined partitioning of the configurational space M. The notion of chemical species can be given a topological definition using these catchment regions [13].

By contrast, there is no universally accepted definition of shape. As a result, the partitioning of space M into shape regions depends on a number of factors: the model chosen to represent the molecular "body" and the chosen shape descriptors. In this work, we have described a number of these possible choices, some of which seem to be detailed enough to lead to significant conclusions on the properties of the shape region partitioning.

In the first place, the potential usefulness of the concept of shape regions has been demonstrated, especially when the shape regions are compared with the catchment regions of the potential energy surface. The two partitionings of space M allow one to recognize the shape types available to a given chemical species. The number and size of the shape regions in configuration space M can give, in principle, a measure of the flexibility and reactivity of a species.

Moreover, studies of molecular shape make it possible to detect essential changes in the electron density which cause no significant change in the potential energy. These changes can be physically meaningful. For example, the occurrence of an interaction between atoms can be revealed by changes in the pattern of the electron density, but it can be hidden when looking for changes in the pattern of the potential energy. A shape region gives a quantitative measure of the configurational subset where these features occur.

It has also been suggested that the size of the cross sections of shape regions found along a conformational or reaction path can provide a measure of the structural similarity between two consecutive species found along the path. This approach appears to be quite promising for addressing several problems involving quantitative assessments of molecular similarity, such as the Hammond postulate, the principle of minimum structure change, and quantitative structure–activity relationships [120].

Several avenues are open for further research. More work with electron density functions is necessary in order to describe in more rigorous terms some of the features revealed by the use of fused-sphere molecular models. From the theoretical point of view, a more satisfactory description of the role of fuzziness in the shape characterization of a surface is not a trivial task. A better description of this problem will result in an improved construction of shape regions. This is likely to give a deeper insight into the notion of molecular shapes accessible to chemical species with different stability or reactivity.

The electron density model of molecular surfaces is practical, in principle, for relatively small molecules. For biomolecules, it is expected that simplified ribbon or space curve models will continue to be used. In the case of biomolecules (proteins, in particular), the detailed study of shape changes along folding paths is only now being undertaken.

Acknowledgements

This work has been supported by strategic and operating research grants from the Natural Sciences and Engineering Research Council (NSERC) of Canada.

References

[1] H. Primas, in: *Quantum Dynamics of Molecules; The New Experimental Challenge to Theorists*, ed. R.G. Woolley, NATO ASI B 57 (Plenum, New York, 1980).

[2] R.G. Woolley, Struct. Bonding 52(1982)1.

[3] F.M. Richards, Ann. Rev. Biophys. Bioeng. 6(1977)151.
[4] R. Langridge, T.E. Ferrin, I.D. Kuntz and M.L. Connolly, Science 211(1981)661.
[5] P.A. Basch, N. Pattabiraman, C. Huang, T.E. Ferrin and R. Langridge, Science 222(1983)1325.
[6] M.L. Connolly, J. Amer. Chem. Soc. 107(1985)1118.
[7] R.S. Pearlman, in: *Partition Coefficient: Determination and Estimation*, ed. W.J. Dunn, J.H. Brock and R.S. Pearlman (Pergamon, New York, 1986).
[8] J.C. McGowan and A. Mellors, *Molecular Volumes in Chemistry and Biology: Applications Including Partitioning and Toxicology* (Horwood, Chichester, 1986).
[9] A.Y. Meyer, Chem. Soc. Rev. 15(1986)449.
[10] H.R. Karfunkel and V. Eyraud, J. Comput. Chem. 10(1989)628.
[11] L. Schäfer, J. Mol. Struct. 100(1983)51.
[12] P.G. Mezey, Molecular surfaces, in: *Reviews in Computational Chemistry*, ed. K.B. Lipkowitz and D.B. Boyd (VCH, New York, 1990).
[13] P.G. Mezey, *Potential Energy Hypersurfaces* (Elsevier, Amsterdam, 1987).
[14] P.G. Mezey, Int. J. Quant. Chem. QBS 12(1986)113.
[15] P.G. Mezey, J. Comput. Chem. 8(1987)462.
[16] G.A. Arteca and P.G. Mezey, Int. J. Quant. Chem. QBS 14(1987)133.
[17] G.A. Arteca and P.G. Mezey, Int. J. Quant. Chem. QBS 15(1988)33.
[18] P.G. Mezey, J. Math. Chem. 2(1988)299.
[19] P.G. Mezey, J. Math. Chem. 2(1988)325.
[20] G.A. Arteca and P.G. Mezey, Int. J. Quant. Chem. QCS 23(1989)305.
[21] G.A. Arteca and P.G. Mezey, J. Phys. Chem. 93(1989)4746.
[22] G.A. Arteca and P.G. Mezey, Int. J. Quant. Chem. 38(1990)713.
[23] W.G. Richards, *Quantum Pharmacology*, 2nd. ed. (Butterworths, London, 1983).
[24] I. Motoc, Steric and other structural parameters for QSAR, in: *Steric Fit in Quantitative Structure–Activity Relationships*, ed. A.T. Balaban, A. Chiriac, I. Motoc and Z. Simon, Lecture Notes in Chemistry No. 15 (Springer, Berlin, 1980).
[25] A.J. Stuper, W.E. Brügger and P.C. Jurs, *Computer-Assisted Studies of Chemical Structures and Biological Function* (Wiley, New York, 1979), ch. 3.
[26] J.M. Blaney, E.C. Jorgensen, M.L. Connolly, T.E. Ferrin, R. Langridge, S.T. Oatley, J.M. Burridge and C.C.F. Blake, J. Med. Chem. 25(1982)785.
[27] R. Franke, *Theoretical Drug Design Methods*, Pharmacochemistry Library, Vol. 7 (Elsevier, Amsterdam, 1977).
[28] J.C. Dearden (ed.), *Quantitative Approaches to Drug Design*, Pharmacochemistry Library, Vol. 6 (Elsevier, Amsterdam, 1983).
[29] R. Bonaccorsi, E. Strocco and J. Tomasi, in: *Chemical and Biochemical Reactivity*, ed. E.D. Bergmann and B. Pullman (Reidel, Dordrecht, 1974).
[30] E. Strocco and J. Tomasi, Topics Curr. Chem. 42(1973)95; Adv. Quant. Chem. 11(1978)115.
[31] J. Tomasi, On the use of electrostatic molecular potentials in theoretical investigations on chemical reactivity, in: *Quantum Theory of Chemical Reactions*, Vol. 1, ed. R. Daudel, A. Pullman, L. Salem and A. Veillard (Reidel, Dordrecht, 1979).
[32] H. Weinstein, R. Osman, J.P. Green and S. Topiol, Electrostcic potentials as descriptors of molecular reactivity, in: *Chemical Applications of Atomic and Molecular Electrostatic Potentisl*, ed. P. Politzer and D.G. Truhlar (Plenum, New York, 1981), pp. 309–334.
[33] J.J. Kaufman, P.C. Hariharan, F.C. Tobi and C. Petrongolo, Electrostatic molecular potential contour maps from ab initio calculations, in: *Chemical Applications of Atomic and Molecular Electrostatic Potentials*, ed. P. Politzer and D.G. Truhlar (Plenum, New York, 1981), pp. 335–380.
[34] A. Pullman and B. Pullman, Electrostatic molecular potential of the nucleic acids, in: *Chemical Applications of Atomic and Molecular Electrostatic Potentials*, ed. P. Politzer and D.G. Truhlar (Plenum, New York, 1981), pp. 381–405.

[35] P. Politzer and K.C. Daiker, Models for chemical reactivity, in: *The Force Concept in Chemistry*, ed. B.M. Deb (Van Nostrand, New York, 1981).
[36] J.R. Rabinowtiz and S.B. Little, Int. J. Quant. Chem. QBS 13(1986)9.
[37] J.C. Culberson, G.D. Purvis III, M.C. Zerner and B.A. Seiders, Int. J. Quant. Chem. QBS 13(1986)267.
[38] G. Náray-Szabó and P.R. Surján, Computational methods for biological systems, in: *Theoretical Chemistry of Biological Systems*, ed. G. Náray-Szabó (Elsevier, Amsterdam, 1986).
[39] G.D. Purvis III and C. Culberson, Int. J. Quant. Chem. QBS 13(1986)216.
[40] R.F. Hout and W.J. Hehre, J. Amer. Chem. Soc. 105(1983)3728.
[41] M.M. Francl, R.F. Hout and W.J. Hehre, J. Amer. Chem. Soc. 106(1984)563.
[42] J.M. Blaney, E.C. Jorgensen, M.L. Connolly, T.E. Ferrin, R. Langridge, S.J. Oatley, J.M. Burridge and C.C.F. Blake, J. Med. Chem. 25(1982)785.
[43] P.K. Weiner, R. Langridge, J.M. Blaney, R. Schaefer and P.A. Kollman, Proc. Nat. Acad. Sci. USA 79(1982)3754.
[44] L.H. Pearl and A. Honegger, J. Mol. Graph. 1(1983)9.
[45] M.L. Connolly, Science 221(1983)709.
[46] M.L. Connolly, J. Mol. Graph. 3(1985)19.
[47] G.A. Arteca and P.G. Mezey, Folia Chim. Theor. Lat. 15(1987)115.
[48] P.G. Mezey, Three-dimensional topological aspects of molecular similarity, in: *Molecular Similarity*, ed. G. Maggiora and M.S. Johnson (Wiley, New York, 1990).
[49] F. Harary, *Graph Theory* (Addison–Wesley, Reading, MA, 1969).
[50] R.J. Wilson and L.W. Beinecke (eds.), *Applications of Graph Theory* (Academic Press, London, 1978)
[51] A.T. Balaban (ed.), *Chemical Applications of Graph Theory* (Academic Press, London, 1976).
[52] N. Trinajstić, *Chemical Graph Theory* (CRC Press, Boca Raton, 1983).
[53] I. Gutman and O.E. Polansky, *Mathematical Concepts in Organic Chemistry* (Springer, Berlin, 1986).
[54] M. Randić, J. Amer. Chem. Soc. 97(1975)6609.
[55] D. Rouvray, J. Comput. Chem. 8(1987)470.
[56] R.B. King (ed.), *Chemical Applications of Topology and Graph Theory* (Elsevier, Amsterdam, 1983).
[57] H. Hosoya and N. Ohkami, J. Comput. Chem. 4(1983)585.
[58] L.B. Kier and L.H. Hall, *Molecular Connectivity in Chemistry and Drug Research* (Academic Press, New York, 1976).
[59] R.E. Merrifield and H.E. Simmons, *Topological Methods in Chemistry* (Wiley, New York, 1989).
[60] M. Randić, Int. J. Quant. Chem. QBS 15(1988)201.
[61] F. Harary and P.G. Mezey, J. Math. Chem. 2(1988)377.
[62] G.A. Arteca and P.G. Mezey, Int. J. Quant. Chem. 34(1988)517.
[63] G.A. Arteca and P.G. Mezey, Theor, Chim. Acta 75(1989)333.
[64] P.G. Mezey, Int. J. Quant. Chem. QBS 14(1987)127.
[65] See, for instance: J.R. Munkres, *Elements of Algebraic Topology* (Addison–Wesley, Menlo Park, 1984);
E.H. Spanier, *Algebraic Topology* (McGraw–Hill, New York, 1966).
[66] G.A. Arteca and P.G. Mezey, J. Comput. Chem. 9 (1988)554.
[67] G.A. Arteca and P.G. Mezey, J. Mol. Struct. 166(1988)11.
[68] P.D. Walker, G.A. Arteca and P.G. Mezey, J. Comp. Chem. 12(1991)220.
[69] J.S. Richardson, Adv. Protein Chem. 34(1981)167.
[70] J.S. Richardson, Meth. Enzymol. 115(1985)359.
[71] M. Carson and C.E. Bugg, J. Mol. Graph. 4(1986)121.
[72] M. Carson, J. Mol. Graph. 5(1987)103.
[73] H. Lass, *Vector and Tensor Analysis* (McGraw–Hill–Kogakusha, Tokyo, 1950).

[74] M. Delbrück, Proc. Symp. Appl. Math. 14(1962)55.
[75] F.B. Fuller, Proc. Symp. Appl. Math. 14(1962)64.
[76] F.B. Fuller, Proc. Nat. Acad. Sci. USA 68(1971)815.
[77] M. Le Bret, Biopolymers 18(1979)1709.
[78] P. De Santis, S. Morosetti and A. Palleschi, Biopolymers 22(1983)37.
[79] M.-H. Hao and W.K. Olson, Biopolymers 28(1989)873.
[80] G.A. Arteca and P.G. Mezey, J. Mol. Graph. 8(1990)66.
[81] G.A. Arteca, O. Tapia and P.G. Mezey, J. Mol. Graph 9(1991)148.
[82] See, for example: R.H. Crowell and R.H. Fox, *Introduction to Knot Theory* (Springer, Berlin, 1977).
[83] K.B. Lipkowitz, B. Barker and R. Larter, J. Amer. Chem. Soc. 111(1989)7750.
[84] R.G. Pearson, *Symmetry Rules for Chemical Reactions, Orbital Topology, and Elementary Processes* (Wiley, New York 1976).
[85] P. Pechukas, J. Chem. Phys. 64(1976)1516.
[86] P.G. Mezey, J. Amer. Chem. Soc. 112(1990)3791.
[87] P.G. Mezey, Non-visual molecular shape analysis: Shape changes in electronic excitations and chemical reactions, in: *Computational Advances in Organic Chemistry*, ed. C. Ögretir and I.G. Csizmadia (Kluwer, Dordrecht, 1991).
[88] G.S. Hammond, J. Amer. Chem. Soc. 77(1955)335.
[89] L. Melander, *The Transition State* (Royal Chemical Society Special Publ., London, 1962).
[90] J.C. Polanyi, J. Chem. Phys. 31(1959)1338.
[91] M.H. Mok and J.C. Polanyi, J. Chem. Phys. 51(1969)1451.
[92] N. Agmon, J. Chem. Soc. Faraday Trans. II 74(1978)388.
[93] A.R. Miller, J. Amer. Chem. Soc. 100(1978)1984.
[94] J.R. Murdoch, J. Amer. Chem. Soc. 105(1983)2667.
[95] G.A. Arteca and P.G. Mezey, J. Comput. Chem. 9(1988)728.
[96] G.A. Arteca, G.A. Heal and P.G. Mezey, Theor. Chim. Acta 76(1990)377.
[97] M.J. Frisch, J.S. Binkley, H.B. Schlegel, K. Raghavachari, C.F. Melius, R.L. Martin, J.J.P. Stewart, F.W. Bobrowicz, C.M. Rohlfing, L.R. Kahn, D.J. Defrees, R. Seeger, R.A. Whiteside, D.J. Fox, E.M. Fleuder and J.A. Pople, *Gaussian'86* (Carnegie-Mellon Quantum Chemistry Publishing Unit, Pittsburgh, 1984).
[98] R.G. Woolley, Chem. Phys. Lett. 125(1986)200.
[99] A. Gavezzotti, J. Amer. Chem. Soc. 105(1983)5220.
[100] G.A. Arteca and P.G. Mezey, *Proc. 11th Conf. IEEE EMBS*, Vol. 11 (1989), p. 1907.
[101] P.K. Pearson, H.F. Schaefer III and U. Wahlgren, J. Chem. Phys. 62(1975)350.
[102] R.A. Poirier, D. Majlessi and T.J. Zielinsky, J. Comput. Chem. 7(1986)464.
[103] X. Luo, G.A. Arteca and P.G. Mezey, Int. J. Quant. Chem., in press.
[104] D.M. Walba, Stereochemical topology, in: *Chemical Applications of Topology and Graph Theory*, ed. R.B. King (Elsevier, Amsterdam, 1983).
[105] V.F.R. Jones, Bull. Amer. Math. Soc. (NS) 12(1985)103.
[106] P. Freyd, D. Yetter, J. Hoste, W.B.R. Lickorish, K. Millett and A. Ocneanu, Bull. Amer. Math. Soc. (NS) 12(1985)239.
[107] D.M. Walba, Tetrahedron 41(1985)3161.
[108] S.A. Wasserman and N.R. Cozzarelli, Science 240(1986)110.
[109] M.L. Connolly, I.D. Kuntz and G.M. Crippen, Biopolymers 19(1980)1167.
[110] T. Kikuchi, G. Némethy and H.A. Scheraga, J. Comput. Chem. 7(1986)67.
[111] J. Simon, J. Comput. Chem. 9(1987)718.
[112] D.W. Sumners, J. Math. Chem. 1(1987)1.
[113] P.G. Mezey, J. Amer. Chem. Soc. 108(1986)3976.
[114] K.C. Millett, J. Comp. Chem. 8(1987)536.
[115] M. Karplus and J.A. McCammon, Ann. Rev. Biochem. 53(1983)263.

[116] F. Colonna-Cesari, D. Perahia, M. Karplus, H. Eklund, C.I. Brändén and O. Tapia, J. Biol. Chem. 261(1986)15273.
[117] O. Tapia, H. Eklund and C.I. Brändén, Molecular, electronic, and structural aspects of the catalytic mechanism of alcohol dehydrogenase, in: *Steric Aspects of Biomolecular Interactions*, ed. G. Náray-Szabó and K. Simon (CRC Press, West Palm Beach, 1987).
[118] P.L. Chau and P.M. Dean, J. Mol. Graph. 5(1987)97.
[119] L. Caccianotti, Istituto "G. Donegani" Preprint, Novara, Italy (1989).
[120] M.A. Johnson, J. Math. Chem. 3(1989)117.